LAPPEENRANTA
UNIVERSITY OF TECHNOLOGY

Markku Kuosa

MODELING REACTION KINETICS AND MASS TRANSFER IN OZONATION IN WATER SOLUTIONS

Thesis for the degree of Doctor of Science (Technology) to be presented with due permission for the public examination and criticism in the auditorium 1383 at Lappeenranta University of Technology, Lappeenranta, Finland on the 18th of December, 2008, at noon.

Acta Universitatis
Lappeenrantaensis
331

Supervisor Professor Juha Kallas
Department of Chemical Technology
Lappeenranta University of Technology
Finland

Reviewers Professor Andrzej K. Bin
Faculty of Chemical and Process Engineering
Warsaw University of Technology
Poland

Professor Bhaskar N. Thorat
University Institute of Chemical Technology
India

Opponent Professor Andrzej K. Bin
Faculty of Chemical and Process Engineering
Warsaw University of Technology
Poland

Custos Professor Juha Kallas
Department of Chemical Technology
Lappeenranta University of Technology
Finland

ISBN 978-952-214-669-4
ISBN 978-952-214-670-0 (PDF)
Lappeenranta University of Technology

Digipaino 2008

Abstract

Markku Kuosa

Modeling reaction kinetics and mass transfer in ozonation in water solutions

Lappeenranta 2008
124 p.
Acta Universitatis Lappeenrantaensis 331
Diss. Lappeenranta University of Technology

ISBN 978-952-214-669-4 ISSN 1456-4491
ISBN 978-952-214-670-0 (PDF)

This dissertation is based on four articles dealing with modeling of ozonation. The literature part of this considers some models for hydrodynamics in bubble column simulation. A literature review of methods for obtaining mass transfer coefficients is presented. The methods presented to obtain mass transfer are general models and can be applied to any gas-liquid system. Ozonation reaction models and methods for obtaining stoichiometric coefficients and reaction rate coefficients for ozonation reactions are discussed in the final section of the literature part.

In the first article, ozone gas-liquid mass transfer into water in a bubble column was investigated for different pH values. A more general method for estimation of mass transfer and Henry's coefficient was developed from the Beltrán method. The ozone volumetric mass transfer coefficient and the Henry's coefficient were determined simultaneously by parameter estimation using a nonlinear optimization method. A minor dependence of the Henry's law constant on pH was detected at the pH range 4 – 9.

In the second article, a new method using the axial dispersion model for estimation of ozone self-decomposition kinetics in a semi-batch bubble column reactor was developed. The reaction rate coefficients for literature equations of ozone decomposition and the gas phase dispersion coefficient were estimated and compared with the literature data. The reaction order in the pH range 7–10 with respect to ozone 1.12 and 0.51 the hydroxyl ion were obtained, which is in good agreement with literature. The model parameters were determined by parameter estimation using a nonlinear optimization method. Sensitivity analysis was conducted using object function method to obtain information about the reliability and identifiability of the estimated parameters.

In the third article, the reaction rate coefficients and the stoichiometric coefficients in the reaction of ozone with the model component p-nitrophenol were estimated at low pH of water using nonlinear optimization. A novel method for estimation of multireaction model parameters in ozonation was developed. In this method the concentration of unknown intermediate compounds is presented as a residual COD (chemical oxygen demand) calculated

from the measured COD and the theoretical COD for the known species. The decomposition rate of p-nitrophenol on the pathway producing hydroquinone was found to be about two times faster than the p-nitrophenol decomposition rate on the pathway producing 4-nitrocatechol.

In the fourth article, the reaction kinetics of p-nitrophenol ozonation was studied in a bubble column at pH 2. Using the new reaction kinetic model presented in the previous article, the reaction kinetic parameters, rate coefficients, and stoichiometric coefficients as well as the mass transfer coefficient were estimated with nonlinear estimation. The decomposition rate of p-nitrophenol was found to be equal both on the pathway producing hydroquinone and on the path way producing 4-nitrocathecol. Comparison of the rate coefficients with the case at initial pH 5 indicates that the p-nitrophenol degradation producing 4-nitrocathecol is more selective towards molecular ozone than the reaction producing hydroquinone. The identifiability and reliability of the estimated parameters were analyzed with the Marcov chain Monte Carlo (MCMC) method.

Keywords: ozonation, bubble column, mass transfer, reaction kinetics, parameter estimation, p-Nitrophenol

UDC 544.4 : 628.16.094.3 -926.214 : 66.023.2 : 544.431.11

Preface

The work leading to the publications presented in this thesis was carried out in the Laboratory of Separation Technology of the Department of Chemical Engineering at Lappeenranta University of Technology during the period of 2004 to 2008.

First of all, I wish to express my sincerest gratitude to my supervisor, Professor Juha Kallas for introducing me into ozonation and for his valuable advice, guidance, and support through out my whole work. I especially wish to thank him for his patience regarding completion of the dissertation.

I thank the Research Foundation of Lappeenranta University of Technology for their financial support.

I would also like to thank Professor Heikki Haario, M.Sc. Antti Solonen for their computational assistance and assisting with writing the articles presented this thesis. I especially wish to thank Dr Arto Laari for his valuable advices and suggestions concerning modeling of mass transfer and reaction kinetics. I also thank him for computational assistance and finally, taking part in writing the articles.

Thanks also go to the pre examiners Professor Andrzej K. Bin from Warsaw University of Technology and Professor Bhaskar Narayan Thorat from University of Mumbai Institute of Chemical Technology.

I would like to thank all my colleagues in the Laboratory of Chemical Engineering (Nowadays, Laboratory of Separation Technology) for their professional support and creating a nice working atmosphere. Special thanks to Mrs Anne Marttinen for all her support and to laboratory engineer Paavo Nurminen for his patience. Thanks go also to Peter Jones for checking the language of this work.

Finally, I wish to express my sincerest appreciation to my wife Mella for her understanding, patience and encouragement to help bring this dissertation to completion. I also wish to thank my sons Nuutti and Antto for ensuring a sense of priority and bringing joy in my life. I would also like to thank my parents, my brother and my sister for their support and interest in my research.

Lappeenranta, September 2008

Markku Kuosa

List of papers

I Kuosa,M., Laari,A.and J. Kallas, "Determination of the Henry's Coefficient and Mass Transfer for Ozone in a Bubble Column at Different pH Values of Water" Ozone Sci. Eng. 26:3 (2004).

II Kuosa, M., Haario, H., Kallas, J., ”Axial Dispersion Model for Estimation of Ozone Self-decomposition” Ozone Sci. Eng. 27:5 (2005)

III Kuosa, Markku; Laari, Arto; Solonen, Antti; Haario, Heikki; Kallas, Juha; Estimation of Multicomponent Reaction Kinetics of p-Nitrophenol Ozonation in a Bubble Column. Industrial & Engineering Chemistry Research (2007), 46(19), 6235-6243

IV Kuosa, Markku; Laari, Arto; Solonen, Antti; Haario, Heikki; Kallas, Juha; Multicomponent reaction kinetics for the ozonation of p-nitrophenol and its decomposition products under acidic conditions at constant pH.
(submitted in July 2008)

Other publications:

Kuosa, M., Kallas, J., Hydrodynamics of dynamic membrane filters, Transactions of The Filtration Society, Volume 2, Issue 3, 2002, p. 61-66

Mänttäri, Mika; Kuosa, Markku; Kallas, Juha; Nyström, Marianne, Membrane filtration and ozone treatment of biologically treated effluents from the pulp and paper industry. Journal of Membrane Science (2008), 309(1+2), 112-119.

M.Kuosa, J.Kallas, Improving the hydrodynamic conditions of dynamic membrane filters, Filtech Europa, Düsseldorf, Germany, 16-18 October 2001, p. 261-268

Kuosa, M., Laari, A., Kallas, J, Ozone mass transfer and self-decomposition in bubble column, International conference on ozone in global water sanitation, Amsterdam, Holland, 1-3 October 2002, p.I-1-1 - I-1-16

Kuosa, M.,Haario, H., Kallas, J.,”Modelling Ozone Mass Transfer and Reaction Kinetics of Ozone Self-decomposition”, International Conference on Advances in Science andf Engineering for Industrial Applications of Ozone and Related Oxidants, Barcelona, Spain, March 10-12 2004, p.I.2.2.-1 - I.2.2-11

Kuosa, M., Laari, A., Kallas, J., Haario, H.," Estimation of Reaction Kinetics in Fast Reaction of Ozone with Organics in Bubble Column: Case: p-Nitrophenol Ozonation". International Conference on Ozone & Related Oxidants, Innovative & Current Technologies, France, Strasbourg, August 22-25 2005, p.IX.2.5-1 - IX.2.5-10

Mika Mänttäri and Markku Kuosa,"Purification of biologically treated water: combination of membrane separation and ozonation", Industrial Water Treatment and Product Purification, 9th CST Workshop, Lappeenranta University of TechnologyLappeenranta, Finland, June 11-14, 2006

Kuosa, M., Kallas, J., "Lignin Ozonation at Different pH values of Water", Environmental Applications of Advanced Oxidation Processes, 1st European conference (EAAOP-1), Chania, 7-9 sep, 2006, Book of abstracts, p. 131, CD-ROM e-proceedings available

Authors contribution

I The author conducted the experimental runs, conducted the analytical work and carried out the modelling under supervision of professor Juha Kallas. Dr Arto Laari assisted with modelling and computation and with writing the article.

II The experimental runs and modelling were conducted by the author under supervision of professor Juha Kallas. Professor Heikki Haario helped with computation and modelling.

III The experimental runs and modelling and some of the analytical work were conducted by author under supervision of professor Juha Kallas. Dr Arto Laari helped with modelling and computation and with writing the article. Professor Heikki Haario and Antti Solonen Msc helped with computational work and with writing the article. The most of the analytical work were conducted by Miss Nieves Calviño.

IV The experimental runs and modelling and the analytical work were conducted by author under supervision of professor Juha Kallas. Dr Arto Laari helped with modelling and computation and with writing the article. Professor Heikki Haario and Antti Solonen Msc helped with computational work and with writing the article. Miss Maribel Fournies conducted a substantial part of the chemical analyses.

Modeling reaction kinetics and mass transfer in ozonation in water solutions

1. Introduction

Ozone has been proven to be very effective chemical for degradation of species which can be poorly degraded in biological waste water treatment. The manufacture of ozone, however, needs a large amount of energy, which makes the optimization of ozonation processes necessary and makes essential both the development of hydrodynamic models, including mass transfer, and development of practicable reaction kinetic models. The chemistry of ozonation in a water solution is rather complex. The reactions of ozonation involve direct molecular reactions of O_3 with dissolved compounds and transformation of O_3 into secondary oxidants such as hydroxyl radicals ($OH^{\bullet}$), hydroperoxyl radicals ($HO_2^{\bullet}$) and further species like $^{\bullet}O_3^-$, $HO_3^{\bullet}$ etc. Modeling of all these reactions requires large amounts of kinetic data, which are not necessarily available or applicable due to the different natures of waters.
In many cases, intermediates from ozone–organic solute reactions are quite well understood, but the reaction schemes and particularly the reaction rate coefficients in the reaction schemes are poorly known. Multicomponent reaction models are thus needed to evaluate reaction rate coefficients and stoichometric coefficients in the reaction schemes.

Bubble column reactors are often used for gas–liquid or gas–liquid–solid reactions because of their efficiency and simplicity. Therefore, a bubble column is also very suitable for ozonation studies. In the simulation of a bubble column, the reactor hydrodynamics model plays a key role. For bubble columns, the hydrodynamics can be presented by using the complete mixing model, the axial dispersion model, the cell model with back flow, and CFD (Computational Fluid Dynamics) models.
In this study, a method was developed to estimate the reaction rate and stoichiometric coefficients of a multi component reaction model in ozonation, taking into account also gas–liquid mass transfer and reactor hydrodynamics. The reaction equations written for the reactions between ozone and the solutes represent ozone decomposition reactions giving the reaction products so that the amount of consumed oxygen calculated from the ozone depletion

meets the stoichiometry needed to oxidize each reactant to products.
Two other methods that could be used for the estimation of the total ozone consumption are based on apparent reaction rate coefficients or the usage of a radical chain reaction mechanism. In the case of a multireaction model, the drawback of the first approach is the high number of rate coefficients and stoichiometric coefficients with a questionable physical meaning due to the danger of over-parameterization. The disadvantage of the radical chain method is the need for a high number of rate coefficients from a number of different authors with different physical and chemical properties of solutions. This latter method has been used by Beltrán et al.,2006, Hautaniemi et al.,1998 and Chelkovska et al.,1992, Kumar et al.,2004 among others.

This thesis reports the results from four articles dealing with ozonation: mass transfer, hydrodynamics, ozone self-decomposition and the multicomponent reaction model. In the literature part of this work, some models for hydrodynamics are briefly considered for bubble column simulation. A concise literature review about methods for obtaining mass transfer coefficients is presented. The methods presented to obtain mass transfer are general models and can be applied to any gas-liquid system. In the final section of the literature part, ozonation reaction models and methods for obtaining stoichiometric coefficients and reaction rate coefficients for ozonation reactions are discussed.

The first article deals with determination of the Henry's coefficient and mass transfer for ozone in a bubble column at different pH values of water. The Henry's coefficient and mass transfer coefficient are estimated by nonlinear parameter estimation using an algebraic mathematical model. The column inlet gas concentration was used as an experimental input variable. The outlet gas concentration and dissolved ozone concentration were used as observed variables.

The second article considers the axial dispersion model for estimation of ozone self-decomposition kinetics in a semi-batch bubble column reactor. The reaction rate coefficients for and gas

dispersion coefficients were estimated and compared with literature data.

In the third article, multicomponent reaction kinetics of p-nitrophenol ozonation were estimated. The axial dispersion model was used to simulation of the hydrodynamics. For estimation both the stoichiometric coefficients and reaction rate coefficients, ozone decomposition reactions were written to give the reaction products so that the amount of consumed oxygen calculated from the ozone depletion is according to the stoichiometry needed to oxidize each reactant to products. It was necessary to include an additional term to take into consideration ozone self-decomposition.
In the fourth article the developed reaction kinetics model was used for estimation of the reaction kinetics of p-nitrophenol ozonation at constant pH 2. The results were compared with the case of p-nitrophenol ozonation without pH adjustment using initial pH 5.
The identifiablity and reliability of the estimated parameters were analyzed in all four articles. In the two first articles the sensitivity analysis was done using sensitivity contour plots of the objective function. In the latter two articles the identifiability and reliability of the estimated parameters were analyzed with the Marcov chain Montecarlo(MCMC) method.

2. Hydrodynamic models for simulation of bubble column

For bubble columns the hydrodynamics can be presented using the complete mixing model, the axial dispersion model, the cell model with back flow, and CFD (Computational Fluid Dynamics) models. The models developed from the complete mixing model are a model of complete mixing in the liquid phase with plug flow in the gas phase and a model of Continuous Flow Stirred Tank Reactors (CFSTR) in series model. In the latter model the gas phase is in plug flow and the liquid phase consists of a series of ideally mixed cells in the axial direction. The CFSTR model is presented in more deatail in chapter 4.1.

2.1 Cell model with back flow

An alternative approach for modelling hydrodynamics and mass transfer in bubble columns is the Cell Model with Backflow (CMB). In this model, multiphase flow is simplified to a cascade of ideally mixed tank reactors in series. In Fig. 1 a flow sheet for CMB is presented (Schlüter et al., 1995) for heat flows. This flow sheet is analogous with the mass transfer case.
A single tank volume in series is

$$V_C = \frac{V_R}{N_C} \qquad \text{with} \quad N_C = \frac{L_R}{H_C} \qquad (2.1)$$

V_R is volume of column and N_C is the number of cells. L_R is the height of the column and H_C is the height of one cell, respectively.
Backflow circulating between neighbouring cells is used to characterise the degree of back-mixing in the partially mixed system. Assuming equidistant cell heights, the backflow ratio, defined as the backflow related to the overall convective volumetric flow rate, can be coupled mathematically with the lumped axial dispersion coefficient of the axial dispersion model:

$$\zeta = \frac{\dot{V}_{G,b}}{\dot{V}_{G,feed}} = \frac{N_C}{Bo_G} - \frac{1}{2} \qquad \text{with} \quad Bo_G = \frac{u_G L_R}{\varepsilon_G D_{eff,G}} \qquad (2.2)$$

$$\gamma = \frac{\dot{V}_{L,b}}{\dot{V}_{L,feed}} = \frac{N_C}{Bo_L} - \frac{1}{2} \qquad \text{with} \qquad Bo_L = \frac{u_L L_R}{\varepsilon_L D_{eff,L}} \qquad (2.3)$$

In equations (2) and (3):

$\dot{V}_{G,b}$ volumetric gas back flow rate, m^3/s

$\dot{V}_{G,feed}$ volumetric gas feed flow rate, m^3/s

Bo_G gas phase Bodenstein number

u_G superficial gas velocity, m/s

ε_G volumetric gas hold up

$D_{eff,G}$ axial gas-phase dispersion coefficient, m^2/s

$\dot{V}_{L,b}$ volumetric liquid back flow rate, m^3/s

$\dot{V}_{L,feed}$ volumetric liquid feed flow rate, m^3/s

Bo_L liquid phase Bodenstein number

u_L superficial liquid velocity, m/s

ε_L volumetric liquid hold up

$D_{eff,L}$ axial liquid-phase dispersion coefficient, m^2/s

Using the energy flows given in Fig. 2.1 an algebraic equation system can be set up for modelling heat transfer and energy distribution in a bubble column reactor. This system of equations must be solved in parallel with mass balances for the gas and liquid phase leading to temperature distribution T(x) on the liquid side over the column height. For mathematical and numerical reasons, the single cell height should not be higher than the reactor diameter. So the number of equidistant cells should be at least

$$N_C \geq \frac{L_R}{D_R} \qquad (2.4)$$

where D_R is the reactor diameter.

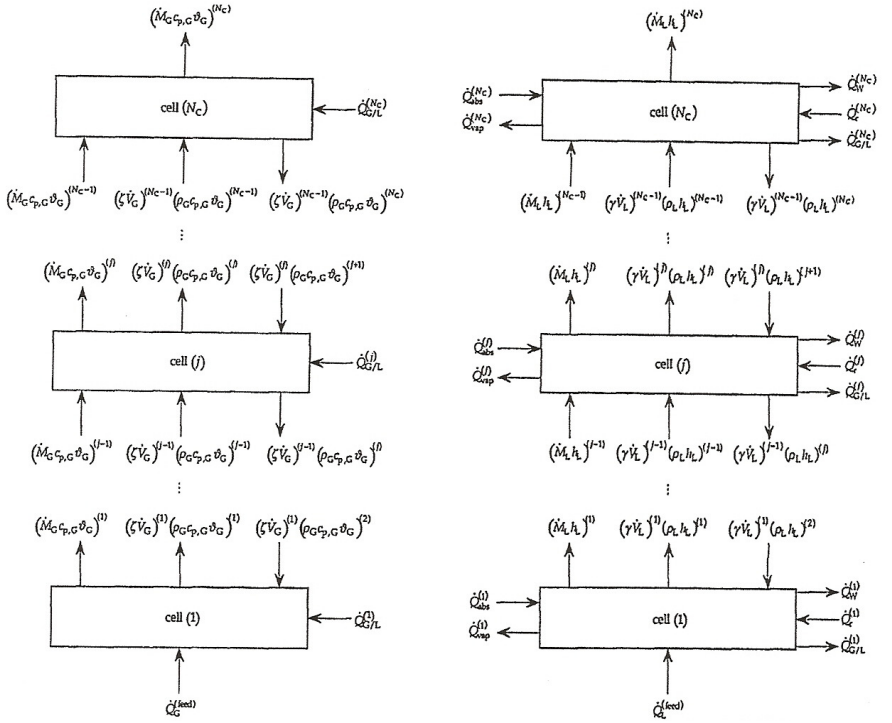

Fig. 2.1 Left: Gas-phase energy flow rates in the cell model with backflow. Right: Liquid-phase energy flow rates in the cell model with backflow. (Schlüter et al., 1995)

2.2 Axial dispersion model

From the physical viewpoint, the Axial Dispersion Model (ADM) is a fully empirical model giving the unknown mixing properties of the system as an axial dispersion coefficient. Nevertheless, the dispersion model can predict gas- and liquid-phase residence time distributions with accuracy sufficient for most technical cases (Schlüter et al.,1992).
For the case of ozone absorption and reaction in the liquid phase ADM can be described mathematically as,

for the gas phase (neglecting ozone decomposition in that phase):

$$\varepsilon_G \frac{\partial [O_3]_G}{\partial t} = -u_G \frac{\partial [O_3]_G}{\partial z} - N_{O_3} + \varepsilon_G D_{eff,G} \frac{\partial^2 [O_3]_G}{\partial z^2} \qquad (2.5)$$

And for the liquid phase:

$$\varepsilon_L \frac{\partial [O_3]_L}{\partial t} = -u_L \frac{\partial [O_3]_L}{\partial z} + N_{O_3} - r_{O_3} + \varepsilon_L D_{eff,L} \frac{\partial^2 [O_3]_L}{\partial z^2} \qquad (2.6)$$

Where

N_{O_3} ozone mass flux, mol/(m^3 s)

r_{O_3} decomposition rate of ozone, mol/(m^3 s)

3. Determination of mass transfer coefficient in a bubble column operated in the semi batch mode

In the example discussed in this chapter the bubble column is operated in semi-batch mode with gas phase flow through an ideally mixed liquid phase. Gas-liquid systems which undergo second order irreversible reactions, as is the case of organic ozonation in water, are used to determine both the liquid phase mass transfer coefficient, $k_L a$, and the reaction rate constant k. Based on film theory (Lewis and Withman, 1924) a stagnant film of thickness L at the surface of the liquid next to the gas is assumed; the rest of the liquid (liquid bulk) far from the film boundary being kept uniform in composition by agitation.

The concentration in the film varies from $[O_3^*]$ at the gas -liquid interface to $[O_3]$ in the bulk of the liquid. The term $[O_3^*]$ is normally taken as the ozone gas solubility because it is assumed that there is no resistance to mass transfer on the gas side of the gas -liquid interface.

Usually the reaction rate of ozone is assumed to be second order, first order for ozone and first order with respect to organics. However, this is not always the case. When a batch reactor is used

and the ozone concentration is changed with time, the reaction order n and the reaction rate constant k_d can be determined in accordance with equation

$$r_{O_3} = \frac{d[O_3]}{dt} = k_d [O_3]^n \qquad (3.1)$$

3.1 Determination of mass transfer coefficient in the slow kinetic regime

In the slow kinetic regime the Hatta number for reaction system of ozone and organics M

$$Ha = \frac{1}{k_L}\left(\frac{2}{1+n} k_{m+n} [M]^m [O_3]^{n-1} D_{O_3}\right)^{1/2} \qquad (3.2)$$

belongs to the range 0.02 < Ha < 0.3 (Charpentier, 1981). The Hatta number indicates the relative importance of the chemical reaction compared to mass transfer and allows to define exactly the absorption kinetic regime. With the condition $[O_3] = 0$ in dissolved phase, the absorption rate of O_3 can be obtained from equation

$$N_{O_3} = k_L a \left[O_3^*\right] \qquad (3.3)$$

Equation 3.3 can be equalized to the disappearance rate of organics M :

$$k_L a \left[O_3^*\right] = z(-d[M]/dt) \qquad (3.4)$$

z is the stoichiometric ratio mol ozone consumed per mol organics. When the term $z(-d[M]/dt)$ is plotted versus $\left[O_3^*\right]$ and a straight line is obtained, the $k_L a$ is equal to the slope. (Beltrán et al., 1992)

3.1.1. Mass transfer in the steady state condition

A steady state is achieved in continuously operated batch reactors if the reaction rate of ozone decomposition is slow enough. In this situation, when the ozone gas feed concentration is kept constant, ozone concentration in the liquid phase rises until a constant steady state value is achieved.
Equation 3.5 can be used for the steady state situation in continuously operated ozone contactors with perfect mixing in the liquid phase.

$$k_L a\left(\left[O_3^*\right]-\left[O_3\right]_{ss}\right)=r_{O_3} \qquad (3.5)$$

Where $[O_3]_{ss}$ is ozone concentration in the liquid phase at the steady state. If r_{O_3}, $[O_3^*]$ and $[O_3]_{ss}$ are known $k_L a$ can be calculated. For an ideally mixed reactor, r_{O_3} can be obtained by calculating directly from the inlet and outlet ozone concentrations of the gas.

3.1.2 Simultaneous determination of mass transfer coefficient and Henry's law constant

If the Hatta number is lower than 0.3 and plug flow of the gas phase and perfect mixing of the water phase are assumed, the following equation can be derived (Beltrán et al., 1995):

$$P_{O_{3o}}=\frac{P_{O_{3i}}}{\exp\left[\dfrac{k_L a\, P_T\, S\, h_T}{H\, m_T}\right]}+\left[H-\frac{H}{\exp\left[\dfrac{k_L a\, P_T\, S\, h_T}{H\, m_T}\right]}\right][O_3] \qquad (3.6)$$

Where

$P_{O_{3o}}$ partial pressure of ozone at the column outlet, Pa

$P_{O_{3i}}$ partial pressure of ozone at the column inlet, Pa

P_T total pressure, Pa

S cross-sectional area of the column, dm^2

h_T height of the column, dm

H apparent Henry's law constant, (Pa dm^3)/mol

$[O_3]$ concentration of dissolved ozone, mol/dm^3

m_T total molar flow rate of gas, mol/s

Equation (3.6) allows simultaneous determination of the mass transfer coefficient $k_L a$ and Henry's law constant H. Thus, a plot of the partial pressure at the reactor outlet, $P_{O_{3o}}$, versus the dissolved ozone concentration $[O_3]$, should yield a straight line whose ordinate ordinate and slope allows $k_L a$ and H to be obtained. With this approach, the ozone inlet concentration (or $P_{O_{3i}}$) should be constant.

3.1.3 Determination of mass transfer coefficient with negligible ozone decomposition

In an ozone contact column with complete mixing, the rate of change of ozone with time can be expressed as

$$\frac{d[O_3]}{dt} = k_L a\left([O_3^*] - [O_3]\right) - r_{O_3} \qquad (3.7)$$

The saturation concentration of ozone and the mass transfer coefficient of the system are measured independently in a solution at a pH where the rate of ozone decomposition is negligible.(Gurol and Singer, 1982)

Equation 10 for this system can be modified to ($r_{O_3} \approx 0$)

$$\frac{d[O_3]}{dt} = k_L a\left([O_3^*] - [O_3]\right) \qquad (3.8)$$

The concentration of ozone is followed with time until the equilibrium concentration of ozone is reached. This concentration

is taken as $[O_3^*]$. $k_L a$ is determined from the slope of the straight line obtained according to the integrated form of equation (3.9)

$$\ln \frac{[O_3^*]-[O_3]}{[O_3^*]-[O_3]_0} = (k_L a)t \qquad (3.9)$$

Where $[O_3]_0$ is the concentration of dissolved ozone at $t = 0$.

3.2 Determination of mass transfer coefficient in the instantaneous kinetic regime

For the instantaneous kinetic regime, the absorption rate of O_3 can be calculated using the equation

$$N_A = k_L a [O_3^*] E_i \qquad (3.10)$$

$$E_i = 1 + \frac{z D_M [M]}{D_{O_3} [O_3^*]} \qquad (3.11)$$

with the condition

$$Ha >> n E_i \qquad (3.12)$$

Where

E_i instantaneous reaction factor

n dimensionless parameter (Danckwerts, 1970)

When the reaction between ozone and organics is instantaneous, the dissolved ozone is completely consumed by the initial organic reactant M, in a plane inside the liquid film (Froment and Bischoff, 1990). Under these conditions ozone is not available for the secondary products at least during the first minutes of

ozonation. Therefore, the ozone absorption rate can be given by equations 3.13 and 3.14 expressed as a function of the disappearance rate of M as follows:

$$N_{O_3} = z\left(-\frac{d[M]}{dt}\right) = k_L a\left[O_3^*\right]\left[1+\frac{z\,D_M[M]}{D_{O_3}\left[O_3^*\right]}\right] \qquad (3.13)$$

D_M is diffusion coefficient of reactant M.

Rearranging and integration of equation 3.13 leads to:

$$\ln\beta = -\left(\frac{D_M k_L a}{D_{O_3}}\right)t \qquad (3.14)$$

Where

$$\beta = \frac{[M]+\dfrac{D_{O_3}\left[O_3^*\right]}{z\,D_M}}{[M]_0+\dfrac{D_{O_3}\left[O_3^*\right]}{z\,D_M}} \qquad (3.15)$$

Where $\left[O_3^*\right]$ can be calculated for an ideally mixed reactor from equations

$$[O_3]_G = \frac{m_f - V_R\, z\left(-\dfrac{d[M]}{dt}\right)_{t=0}}{\dot{V}_G} \qquad (3.16)$$

$$\left[O_3^*\right] = \frac{[O_3]_G RT}{H} \qquad (3.17)$$

Where

$[O_3]_G$ ozone concentration at the outlet of reactor, mol/dm^3

m_f ozone molar flow rate at the reactor inlet, mol/s

A plot of the left-hand side of equation 3.14 versus time leads to a straight line. $k_L a$ can be calculated from the slope $-\frac{D_M\, k_L a}{D_{O_3}}$.

3.3 Mass transfer in the fast kinetic regime with pseudo first order reactions

3.3.1 Estimation at the initial rate

A condition for a fast pseudo first order reaction is $3 < Ha < E_i / 2$. The absorption rate of ozone can be expressed as function of the organic M consumption rate once the stoichiometry is accounted for:

$$N_{O_3,t=0} = a\left[O_3^*\right]\left(k_{O_3}\, D_{O_3}\left[M\right]_0\right)^{1/2} = z\left(\frac{d[M]}{dt}\right)_{t=0} \qquad (3.18)$$

Where $t = 0$ means that only the initial rate of decomposition is taken into consideration and ozone consumption by intermediate products, which affects ozone stoichiometry, is neglected. According to Beltran et al. (1992) $\left[O_3^*\right]$ can be calculated using equations 3.16 and 3.17. Based on equation 3.18 a plot of $z\left(\frac{d[M]}{dt}\right)_{t=0}$ versus $\left[O_3^*\right]\left([M]_0\right)^{1/2}$ should yield a straight line provided the ozonation reactions follow the fast pseudo first order kinetic regime. If the reaction rate coefficient k_{O_3} is known, the specific interfacial area a can be calculated from the slope $a\left(k_{O_3}\, D_{O_3}\right)$.

3.3.2 Estimation of the specific interfacial area or rate coefficient from inlet gas and outlet gas concentration data

The following ozone balance equation can be written for a volume differential element (Figure 3.1)

$$-\frac{m_T}{P_T} dP_{O_3} = N_{O_3} \beta S\, dh + \frac{d[O_3]_G}{dt} S\, dh \qquad (3.19)$$

Where β is liquid hold-up. N_{O_3} depends on physico -chemical parameters (rate and mass transfer coefficients) and concentrations. For the fast pseudo first order kinetic regime, equation 3.18 applies for the reaction between ozone and COD. In the following equations 3.20 – 3.28 the symbol M could be used in place of COD, respectively. However, COD is more appropriate in presentation of ozone flux because by using COD instead of M the effect of intermediates on flux need not to be taken into consideration.

$$N_{O_3} = a\left[O_3^*\right]\sqrt{k_{O_3} COD\, D_{O_3}} \qquad (3.20)$$

Where according to Henry's law

$$\left[O_3^*\right] = \frac{P_{O_3}}{H} \qquad (3.21)$$

By substituting N_{O_3} from equation 3.20 into equation 3.19, taking into account the Henry and gas perfect laws for $\left[O_3^*\right]$ and $d[O_3]_G$ respectively, the ozone mole balance becomes as follows:

$$-\frac{m_T}{P_T} dP_{O_3} = a\frac{P_{O_3}}{H}\beta\sqrt{k_{O_3} COD\, D_{O_3}}\, S dh + \frac{dP_{O_3}}{dt}\frac{S}{RT} dh \qquad (3.22)$$

Equation 3.22 can be simplified by neglecting the accumulation rate term, which has been found to be at least 1000 times lower than the left side equation term (García-Araya, 1993). Thus the

resulting equation, after variable separation, can be integrated with the following boundary conditions:

$$h = 0 \qquad P_{O_3} = P_{O_{3i}} \tag{3.23}$$

$$h = h_T \qquad P_{O_3} = P_{O_{3o}} \tag{3.24}$$

to give:

$$\ln \frac{P_{O_{3i}}}{P_{O_{3o}}} = \frac{a\, P_T \beta\, S \sqrt{k_{O_3} D_{O_3}}}{H\, m_T} h_T \sqrt{COD} \tag{3.25}$$

where $P_{O_{3i}}$ and $P_{O_{3o}}$ are partial pressures at the inlet and at the outlet of the column.

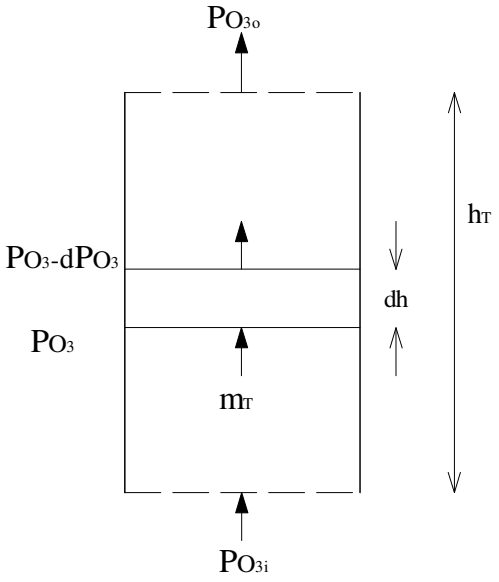

Figure 3.1 Volume differential element in a bubble column.

Krevelen and Hoftijer (1948) derived a more general equation, 3.26, which is valid for fast, moderate or slow reactions and can be used for the mass transfer rate instead of equation 3.20.

$$N_{O_3} = k_L a \left[O_3^*\right]_L \frac{Ha}{\tanh Ha}\left(1 - \frac{k_L a \dfrac{Ha}{\sinh Ha \cosh Ha}}{(1-\varepsilon_G)k_{O_3} COD + k_L a \dfrac{Ha}{\tanh Ha}}\right) \qquad (3.26)$$

In the case of fast reaction equation 3.26 reduces to

$$N_{O_3} = k_L a \left[O_3^*\right]_L Ha \qquad (3.27)$$

and into

$$N_{O3} = k_{O_3} \left[O_3^*\right] COD(1-\varepsilon_G) \qquad (3.28)$$

in the case of a very slow reaction.

4. Experimental determination of mass transfer coefficient for the continuous-flow countercurrent ozone contactor

The mass balance of the gaseous ozone in the reactor can be written as follows

$$\dot{V}_G([O_3]_{Gi} - [O_3]_{Go}) = V_R k_L a(\left[O_3^*\right]_L - [O_3]_L) \qquad (4.1)$$

Thus $k_L a$ can be calculated for an ideally mixed reactor as

$$k_L a = \frac{\dot{V}_G([O_3]_{Gi} - [O_3]_{Go})}{V_R(\left[O_3^*\right]_L - [O_3]_L)} = \frac{\dot{V}_G([O_3]_{Gi} - [O_3]_{Go})}{V_R(S[O_3]_{Go} - [O_3]_L)} = \frac{R_{O_3}}{(S[O_3]_{Go} - [O_3]_L)} \qquad (4.2)$$

Where

S is solubility ratio

R_{O_3} is the rate of ozone mass transfer g/(dm^3 s)

The general mass transfer equation proposed by Danckwerts (1970) when applied to ozone mass transfer results in the following expression

$$R_{O_3} = k_L a\sqrt{1+Ha^2}\left(\left[O_3^*\right]_L - \frac{[O_3]_L}{1+Ha^2}\right) \qquad (4.3)$$

If the value of Ha^2 is low enough, equation 4.3 is indistinguishable from equation 4.2 and mass transfer enhancement can be neglected (Kumar and Bose,2004, Zhou et al., 1994).

4.1 Determination of mass transfer coefficient and kinetic constant by optimization

Roustan et al. (1996) estimated mass transfer and reaction rate constant for ozone for both co-current and counter current flow in a bubble column. Their findings always resulted in higher values of $k_L a$ for counter current mode than that for co-current mode. They assumed plug flow behaviour for the gas phase and the liquid phase behaviour as a series of equally-sized well mixed reactors (Figure 4.1).

Mass balance for the gas phase for the i^{th} reactor is:

$$[O_3]_{Gi} - [O_3]_{Gi-1} + \frac{V_{Ri}}{V_G} k_L a \frac{m([O_3]_{Gi-1} - [O_3]_{Gi})}{\ln\left(\frac{m[O_3]_{Gi-1} - [O_3]_{Li}}{m[O_3]_{Gi} - [O_3]_{Li}}\right)} = 0 \qquad (4.4)$$

Mass balance for the liquid phase for the i^{th} reactor

$$[O_3]_{Gi} - [O_3]_{Gi-1} + \frac{V_L}{V_G}([O_3]_G - I_{cc}[O_3]_{Li+1} - (1-I_{cc})[O_3]_{Li-1}) + \frac{V_{Ri}}{V_G} k[O_3]_{Li} \qquad (4.5)$$

$I_{cc} = 1$ for counter current flow and $I_{cc} = 0$ for co-current flow

If j is the number of well mixed reactors, the size of the model to be solved is $2\times j$, the observed variables being $[O_3]_{Gi}$ and $[O_3]_{Li}$ for $i=1\ to\ j$. Roustan et al. estimated parameters k_La and k using the Gauss-Newton method in order to minimize a least square criterion as an object function

$$l(k_La,k)=\sum_{k=1}^{n_L}\left(\frac{[O_3]_{L_{k,m}}-[O_3]_{L_{k,p}}}{[O_3]_{L_{k,m}}}\right)^2+\sum_{k=1}^{n_G}\left(\frac{[O_3]_{G_{k,m}}-[O_3]_{G_{k,p}}}{[O_3]_{G_{i,m}}}\right)^2 \qquad (4.6)$$

where

n_L and n_G are the numbers of liquid and gas phase observations for ozone concentrations in outlet streams of the column. $[O_3]_{L_{k,m}}$ and $[O_3]_{G_{k,m}}$ are the measured ozone concentrations in the outlet streams. $[O_3]_{L_{k,p}}$ and $[O_3]_{G_{k,p}}$ are model-predicted ozone concentrations in the outlet streams.

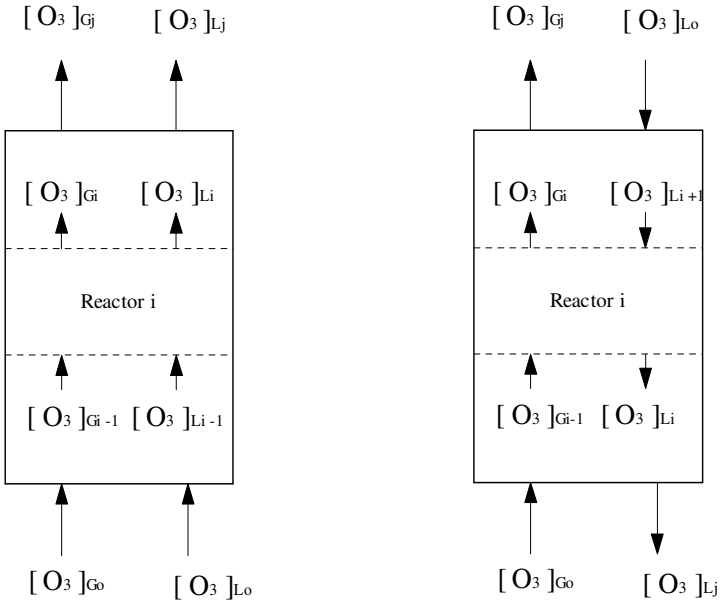

Figure 4.1 Schematic diagram of co-current and counter current columns.

5. Empirical and semi-empirical and theoretical correlations of k_La, k_L and a

A large number of empirical and semi-empirical correlations concerning mass transfer can be found in the literature. Phase superficial velocities, reaction rate, ionic strength, temperature, pH and impurities in general affect k_La. In different liquids there are different k_La values (Akita and Yoshida, 1973), and gas properties affect on k_La as well (Öztürk et al.,1987). The operation mode of the column (co-current or counter current) also affects on k_La. It is almost impossible to find a correlation for k_La which takes all factors into consideration. In general, extreme care must be taken in the use of empirical correlations. They are, however, often useful as first guess approximations.
Knowledge of k_L permits evaluation of the importance of the effect of the chemical reaction affecting on mass transfer. Higbie (Danckverts, 1970) has proposed the equation

$$k_L = 1.13\sqrt{\frac{D}{t_c}} \qquad (5.1)$$

where t_c is the contact time calculated by using the following equation

$$t_c = \frac{d_B}{U_S} \qquad (5.2)$$

Where d_B is the bubble diameter, and U_S us the rise velocity of the bubble with respect to the liquid.

For bubble columns with ultrapure water, Calderbank's equation (Froment and Bischoff, 1979), which does not take the superficial velocity of gas into consideration at all, is

$$k_L = 0.42\sqrt{\frac{\mu_L\, g}{\rho_L}}\sqrt{\frac{\rho_L D_{O_3}}{\mu_L}} \quad , \quad d_B \geq 2.0\times10^{-3} \quad m \qquad (5.3)$$

$k_L a$ correlation equations are usually functions of gas superficial velocity. Various relationships of the form

$$k_L a = a U_G{}^{b} \qquad (5.4)$$

have been presented for estimation of $k_L a$ in bubble column reactors. For example, Laplanche et al.(1989) gave the following equation for ozonation at 20 °C

$$k_L a = 7.91\times10^{-4} U_G{}^{0.54} \qquad (5.5)$$

Bin and Roustan (2000) presented a collection of empirical correlations of the form of equation 5.4.

The specific interfacial area a is an important design variable which is related to gas holdup ε_G and the diameter of bubbles as follows

$$a = \frac{6}{d_B}\frac{\varepsilon_G}{1-\varepsilon_G} \qquad (5.6)$$

Different photographic techniques and image analysis methods can be used to obtain d_B.

6. Decomposition of ozone

The stability of the aqueous ozone is affected by pH, ultraviolet light, ozone concentration and concentration of radical scavengers (Tomiyasu et al., 1985). The decomposition rate, measured in the presence of an excess of radical scavengers which prevent secondary reactions, is expressed by a pseudo first order kinetic equation of the following configuration:

$$-\frac{d[O_3]}{dt} = k'[O_3]^1 \qquad (6.1)$$

and

$$\ln\frac{[O_3]}{[O_3]_0} = k't \qquad (6.2)$$

where k' is a pseudo first order rate constant for a given pH value.
The pseudo first order constant is a linear function of pH as shown in Figure 6.1. This evolution reflects that the ozone composition rate is first order with respect to both ozone and hydroxide ions, resulting in an overall equation of the following form:

$$-\frac{d[O_3]}{dt} = k[O_3][OH^-] \qquad (6.3)$$

Where $k = \frac{k'}{[OH^-]}$ (6.4)

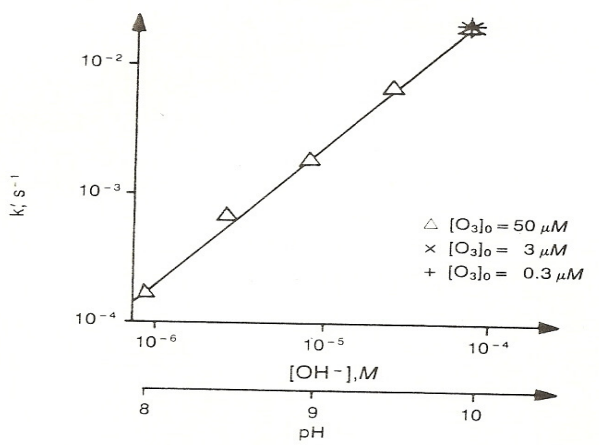

Figure 6.1 Pseudo first order rate coefficient as a function of hydroxide ion concentration (Langlais et al., 1991).

In the ozonation of natural waters the first order law is not always correct (Gurol and Singer, 1982; Yurteri and Gurol, 1988; Tomiyasu et al., 1985) According to Tomiyasu et al.(1985) for example, in some cases at pH 8-11, a combined first- and second-order rate law is more correct.

$$-\frac{d[O_3]}{dt} = k_w[O_3] \qquad (6.5)$$

where $k_w = a + b\exp(c\,\Delta[O_3])$ (6.6)

where a, b, and c are kinetic parameters, and $\Delta[O_3]$ refers to the change in ozone concentration.

6.1. Chain reaction models for decomposition of ozone

Ozone decomposition occurs in a chain reaction process that in literature is presented with different series of reactions. In practice, there are two dominating reaction chain models: the HSB (Hoigné,Staehelin and Bader) mechanism and the GTF (Gordon, Tomiyasu and Fukutomi) mechanism. The HSB model is valid for neutral or near neutral conditions. The GTF model has been verified with pulse radiolysis at high pH levels (pH > 10). The HSB mechanism can be presented by the following fundamental reactions (Weiss, 1935,Staehelin 1984). This mechanism is also presented in Fig. 6.2.

$$O_3 + OH^- \longrightarrow HO_2^\bullet + O_2^- \qquad k = 7.0\times10\ M^{-1}s^{-1} \qquad (6.7)$$

$$HO_2^\bullet \longleftrightarrow {}^\bullet O_2^- + H^+ \qquad k_a = 10^{4.8} \qquad (6.8)$$

$$O_3 + {}^\bullet O_2^- \longrightarrow {}^\bullet O_3^- + O_2 \qquad k = 1.6\times10^9\ M^{-1}s^{-1} \qquad (6.9)$$

$$^\bullet O_3^- + H^+ \longleftrightarrow HO_3^\bullet \qquad k = 5.2\times10^{10}\ M^{-1}s^{-1} \qquad (6.10)$$

$$k_- = 2.3\times10^2\ s^{-1}$$

$$HO_3 \longrightarrow OH^\bullet + O_2 \qquad k = 1.1\times10^3\ s^{-1} \qquad (6.11)$$

$$OH^\bullet + O_3 \longrightarrow HO_4 \qquad k = 2.0\times10^9\ M^{-1}s^{-1} \qquad (6.12)$$

$$HO_4 \longrightarrow HO_2^\bullet + O_2 \qquad k = 2.8\times10^4\ s^{-1} \qquad (6.13)$$

$$HO_4 + HO_4 \longrightarrow H_2O_2 + 2O_3 \qquad (6.14)$$

$$HO_4 + HO_3^\bullet \longrightarrow H_2O_2 + O_3 + O_2 \qquad (6.15)$$

In the initiation step of the HSB model, the reaction between OH^- ions and ozone leads to the formation of one superoxide anion

$^{\bullet}O_2^-$ and one hydroperoxyl radical $HO_2^{\bullet}$ which are in acid base equilibrium ($pK_a = 4.8$).

The GTF-mechanism involves a two-electron transfer process or an oxygen atom transfer from ozone to the hydroxide ion (Tomiyasu et al., 1985, Grasso, 1987, Gordon, 1987). In this mechanism $HO_3^{\bullet}$ and HO_4 are not proposed. In Hoignés mechanism, if these species agree with the mechanistic pathway, some additional experiments may be necessary to confirm their existence. The GTF ozone decomposition mechanism is presented with the following steps:

$$O_3 + OH^- \longrightarrow HO_2^- + O_2 \qquad k = 40 \pm 2\ M^{-1}s^{-1} \qquad (6.16)$$

$$HO_2^- + O_3 \longrightarrow {}^{\bullet}O_3^- + HO_2^{\bullet} \qquad k = 2.2\times10^6\ M^{-1}s^{-1} \qquad (6.16)$$

$$HO_2^{\bullet} + OH^- \longleftrightarrow {}^{\bullet}O_2^- + H_2O \qquad k_a = 10^{-4.8} \qquad (6.17)$$

$$^{\bullet}O_2^- + O_3 \longrightarrow {}^{\bullet}O_3^- + O_2 \qquad k = 1.6\times10^9\ M^{-1}s^{-1} \qquad (6.18)$$

$$^{\bullet}O_3^- + H_2O \longrightarrow OH^{\bullet} + O_2 + OH^- \qquad k = 20-30\,M^{-1}s^{-1} \qquad (6.19)$$

$$^{\bullet}O_3^- + OH^{\bullet} \longrightarrow {}^{\bullet}O_2^- + HO_2^{\bullet} \qquad k = 6\times10^9\ M^{-1}s^{-1} \qquad (6.20)$$

$$O_3 + OH^{\bullet} \longrightarrow O_3 + OH^- \qquad k = 2.5\times10^9\ M^{-1}s^{-1} \qquad (6.21)$$

$$OH^{\bullet} + O_3 \longrightarrow HO_2^{\bullet} + O_2 \qquad k = 3\times10^9\ M^{-1}s^{-1} \qquad (6.22)$$

$$OH^{\bullet} + CO_3^{2-} \longrightarrow OH^- + CO_3^- \qquad k = 4.2\times10^8\ M^{-1}s^{-1} \qquad (6.23)$$

$$CO_3^- + O_3 \longrightarrow products(CO_2 + O_2^- + O_2) \qquad (6.24)$$

6.1.1 Hydrogen peroxide

Hydrogen peroxide H_2O_2 is a weak acid. It is produced in the radical chain. In water solution, it partially dissociates into hydroperoxide ion HO_2^-.

$$H_2O_2 + H_2O \longleftrightarrow HO_2^- + H_2O^+ \qquad k_a = 10^{-11.6} \qquad (6.25)$$

The hydrogen peroxide molecule reacts very slowly with ozone (Taube and Bray 1940), whereas the hydrogenperoxide anion is highly reactive. As a result, the ozone decomposition rate by hydrogen peroxide increases with increasing pH.
It has been shown that the ozone decomposition with hydrogen peroxide can be presented by a second order kinetic equation (Langlais et al., 1991, Kuo et al., 1997 , Beltrán , 2004)

$$-\frac{d[O_3]}{dt} = k''[O_3][HO_2^-] \qquad k'' = 5.5 \pm 1.0 \times 10^6\ M^{-1}s^{-1} \qquad (6.26)$$

The rate constant k'' is vastly superior to that of ozone decomposition initiated by hydroxyl ions. Therefore, the result is that very low concentrations of HO_2^- are kinetically effective in initiating O_3 decomposition.
Based on the mechanism of ozone decomposition, the initiation and propagation reactions could be as follows (Langlais et al., 1991)

$$H_2O_2 + H_2O \longleftrightarrow HO_2^- + H_2O^+ \qquad k_a = 10^{-11.6} \qquad (6.27)$$

$$O_3 + HO_2^- \longrightarrow OH^\bullet + {}^\bullet O_2^- + O_2 \qquad k = 2.2 \times 10^6\ M^{-1}s^{-1} \qquad (6.28)$$

$$O_2^- + H^+ \longleftrightarrow HO_2^\bullet \qquad 1/k_a = 10^{4.8} \qquad (6.29)$$

$$O_3 + {}^\bullet O_2^- \longrightarrow {}^\bullet O_3^- + O_2 \qquad k = 1.6 \times 10^9\ M^{-1}s^{-1} \qquad (6.30)$$

$$^{\bullet}O_3^- + H^+ \longleftrightarrow HO_3^{\bullet} \qquad k = 5.2\times10^{10}\ M^{-1}s^{-1} \qquad (6.31)$$

$$k_{-} = 2.3\times10^{2}\ s^{-1}$$

$$HO_3^{\bullet} \longrightarrow OH^{\bullet} + O_2 \qquad k = 1.1\times10^{5}\ s^{-1} \qquad (6.32)$$

6.2 Initiators, promoters, and inhibitors of free radical reactions

The hydroxide ion plays a fundamental role in initiating the ozone decomposition process. In fact, a wide variety of compounds are able to initiate, promote or inhibit the chain reaction processes (Hoigné and Bader, 1977 a; Staehelin and Hoigné, 1983).

The initiators of the free radical reaction, that is, the compounds capable of inducing the formation of the superoxide ion $^{\bullet}O_2^-$ from an ozone molecule, are inorganic compounds (for example hydroxyl ions OH^-, hydroperoxide ions HO_2^- and some cations) and organic compounds (for example glyoxylic acid, formic acid and humic substances). Ultraviolet radiation at 253.7 nm is also capable of initiating the free radical process.

The promotors of the free-radical reaction are organic and inorganic molecules capable of regenerating the $^{\bullet}O_2^-$ from the hydroxyl radical $^{\bullet}OH$. Common promotors are organics with aryl groups, formic acvid, glyoxylic acid, primary alcohols and humic acids.

The inhibitors of free radical reaction are compounds capable of consuming $^{\bullet}OH$ without regenerating $^{\bullet}O_2^-$. Some of the more common inhibitors are bicarbonate an carbonate ions, alkyl groups, tertiary alcohols and humid substances (Hoigné and Bader, 1985).

6.3 Ozone reactions with organics

In water solution ozone reacts with organic molecule by direct reaction or by radical-type reaction.
For direct reaction of ozone with a solute M can be written

$$\gamma O_3 + M \longrightarrow M_{ox} \qquad (6.33)$$

where γ is a stoichiometric factor for the number of ozone molecules consumed per molecule M transformed to oxidized molecule M_{ox}.

6.3.1 Reaction kinetics of the ozone-solute reaction

The decomposition rate of ozone in an ozone – organic matter M reaction is generally presented with second order equation (Hoigné and Bader, 1981).

$$r_{O_3,i} = \left(\frac{d[O_3]}{dt} \right)_i = \gamma_i k_i [O_3][M] \qquad (6.34)$$

where $r_{O_3,i}$ is the decomposition rate of ozone in reaction i, and γ_i is the stoichiometric coefficient, the number of moles of ozone consumed per moles of decomposed M.
The reaction of ozone with inorganic compounds generally follows the first order kinetic law with respect to ozone and the oxidable compound resulting in a similar second order reaction rate equation to equation 6.34.

The acidic organic molecule M can dissociate in the form

$$M \longleftrightarrow M^- + H^+ \qquad (6.35)$$

Thus, the disappearance rate of ozone can be written as

$$r_{O_3,i,i-} = \gamma_{i,i-} k_{i,i-} [O_3][M]_{TOT} = r_{O_3,i-} + r_{O_3,i} = \gamma_{i-} k_{i-} [O_3][M^-] + \gamma_i k_i [O_3][M] \qquad (6.36)$$

where γ_{i-} and $k_{O_3,-}$ are the stoichiometric coefficient and the rate coefficient for the ionic form of M.
The overall reaction rate for the oxidation of acidic substances strongly depends on the degree of dissociation, and consequently, on the pH of the solution.
The decomposition rate of solute M related to equations 6.35 and 6.36 is

$$\left(\frac{d[M]}{dt}\right)_i = k_i[O_3][M] \qquad (6.37)$$

In some cases, the decomposition rate of the solute is presented as a summation of the rates of the direct reaction by ozone and the indirect reaction by the hydroxyl radical $OH^{\bullet}$(Gurol and Nekouinaini, 1984)

$$\frac{d[M]}{dt} = k[O_3][M] + k'[OH^{\bullet}][M] \qquad (6.38)$$

Hydroxyl radical concentration cannot be measured directly. Consequantly, an O_3 resistant $OH^{\bullet}$ probe compound is usually used, for example, para-chlorobezoic acid (pCBA).

6.3.2 Role of organics in the radical chain reaction

Accoring to Staehelin and Hoigné (1985) solutes M may react with ozone and consume ozone by direct reaction (d) or produce an ozonide ion radical $^{\bullet}O_3^-$ by electron transfer (d')(in the initiation step). The other path in the initiation step is the reaction of ozone with the hydroxide ion OH^-, See Figure 6.2. Upon protonation $^{\bullet}O_3^-$ decomposes into $OH^{\bullet}$ radicals. These react with solutes M. Some functional groups present in organic molecules M are known to react with $OH^{\bullet}$ to form an organic radical which adds O_2 and then eliminates $HO_2^{\bullet}/^{\bullet}O_2^-$ in a base-catalyzed reaction and

as a result M is oxidised (11)(in the propagation step). Many organic and inorganic substrates react with $OH^{\bullet}$ radicals to form such secondary radicals which do not predominantly produce $HO_2^{\bullet}/^{\bullet}O_2^{-}$. These scavengers generally terminate the chain reaction (8) (the termination step).

Pi et al.(2005) suggested an additional reaction pathway in which $OH^{\bullet}$ radicals , or in some cases aqueous ozone, attack aromatic rings and lead to the formation of olefins. Then the reaction of ozone with the olefins leads to production of hydrogen peroxide. Parts of the hydrogen peroxide dissociate to HO_2^{-}, which has a much higher initiating ability than OH^{-}. The formation and location of olefins in the radical chain is presented in Fig. 6.3.

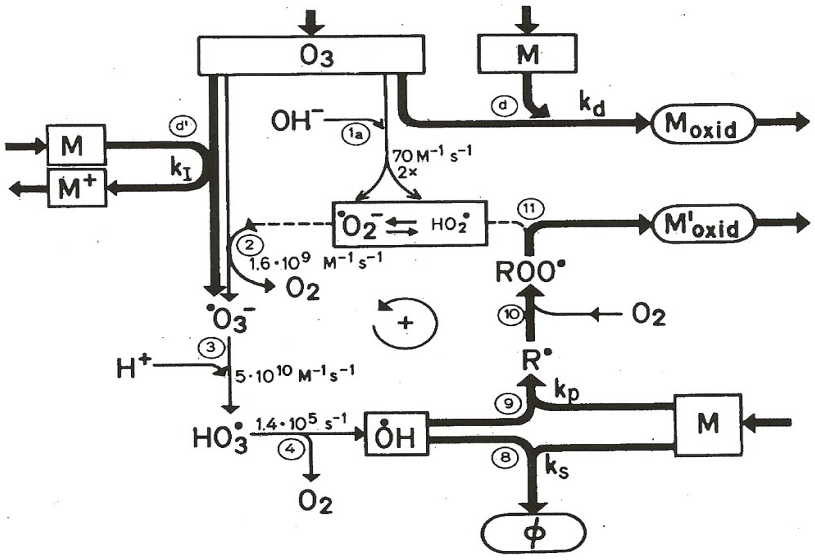

Figure 6.2 Reactions of aqueous ozone in the presence of solutes M which react with O_3 or interact with $^{\bullet}OH$ radicals by scavenging and/or converting $^{\bullet}OH$ into $HO_2^{\bullet}$.(Staehelin and Hoigné, 1985)

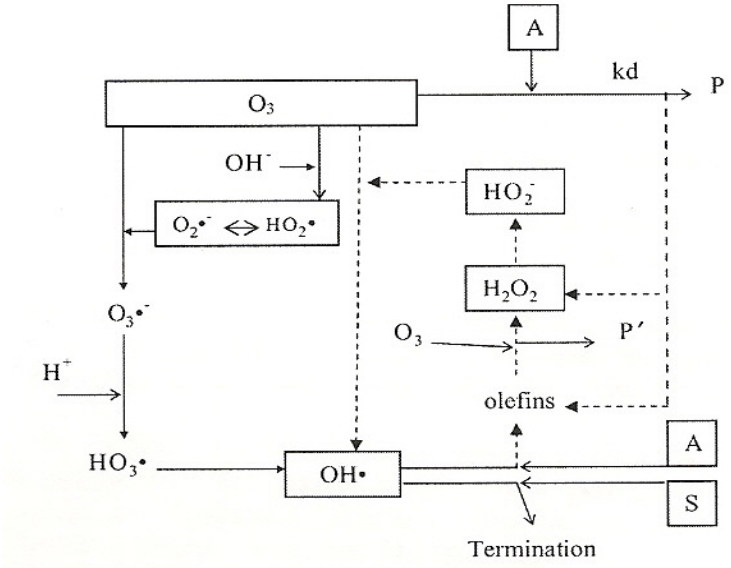

Figure 6.3 An assumed reaction pathway of aromatic compounds with aqueous ozone. Aromatic compounds (A), scavenger (S), oxidation products (P and P′). (Pi et al., 2005)

6.3.3. Molecular structure and reactivity with ozone

The two ozonolysis pathways are 1)direct attack electrophilic or dipolar cyclo addition and 2)indirect attack by free radicals produced by a reaction with water and water constituents.
Initial molecular reaction sites are either multiple bonds $C=C$, $C=C-O-R$, $-C=C-X$ or atoms carrying a negative charge N, P, O, S and nucleophilic carbons. A strong initial reactivity is therefore predicted for ortho-activated aromatics by substituents such as OH, CH_3, OCH_3. A weaker initial reactivity is predicted for molecules with NO_3, CO_2H and CHO groups. Radical reactions (for example reactions of $OH^{\bullet}$) are unselective.

6.3.4 Rate constants for substituted benzenes

Benzene and substituted benzenes are important in waste water ozonation research because they are often used as model compounds. The reaction rate constants of different substituted benzenes vary by many orders of magnitude (Table by Hoigné and Bader (1983) on page 44). A linear relationship is obtained for $\log_{10}\frac{k}{k_0}$ vs. the Hammet-Brown constant σ_p^+ (Exner, 1972, Hoigné and Bader, 1983). This is presented in Fig. 6.4. k_0 is the rate constant for the reference component (benzene) and k is the rate constant for the component itself.

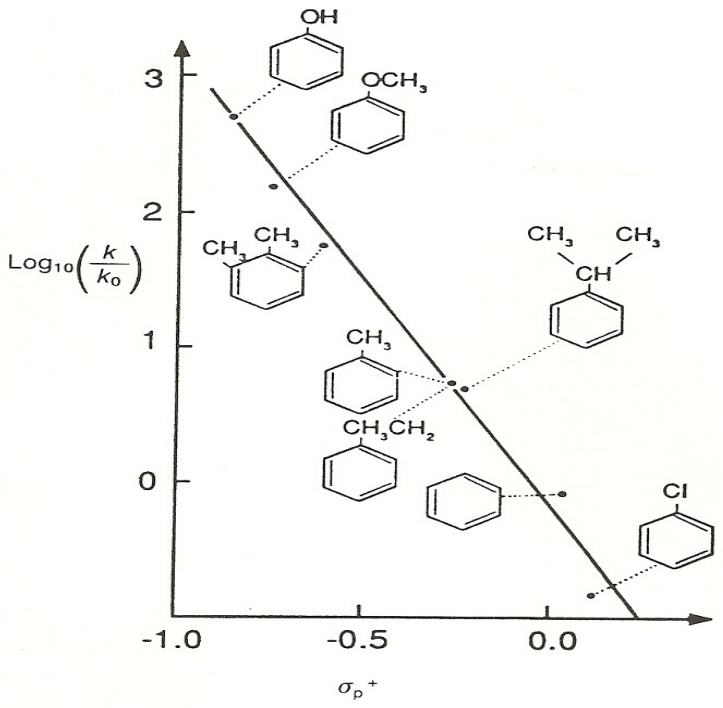

Figure 6.4 Stock-Brown plot of substituted benzenes. (Hoigné and Bader, 1977)

Reaction-rate constants of phenols (HB) and phenolate ions (B^-)¶

Solute	pK_{HB}	mM	pH range	Scavenger	mM	k_{HB} ($M^{-1}s^{-1}$)	k_{B^-} ($M^{-1}s^{-1}$)	(N)†	calc. k_{tot} for pH = 8 ($M^{-1}s^{-1}$)
Phenol	9.9	$(0.4–4)\ 10^{-2}$	2–6	*t*-BuOH	3	$1.3 \pm 0.2 \cdot 10^3$	$1.4 \pm 0.4 \cdot 10^9$	(17)	$18 \cdot 10^6$
2-Chlorophenol	8.3	0.004–1	1.8–4	*t*-BuOH	3	$1.1 \pm 0.3 \cdot 10^3$	$0.2 \pm 0.1 \cdot 10^9$	(16)	$66 \cdot 10^6$
4-Chlorophenol	9.2	0.002–1	1.5–6	*t*-BuOH	3	600 ± 100	$0.6 \pm 0.2 \cdot 10^9$	(30)	$34 \cdot 10^6$
2,3-Dichlorophenol	7.7	0.03–0.3	2	*t*-BuOH	3	$<2 \cdot 10^3$		(6)	
2,4-Dichlorophenol	7.8**	0.03–0.3	1.5–3	*t*-BuOH	3	$<1.5 \cdot 10^3$	$\sim 8 \pm 4 \cdot 10^9$	(9)	$\sim 5 \cdot 10^9$
2,4,6-Trichlorophenol	6.1**	0.2–0.3	1.3–1.5	*t*-BuOH	3	$<10 \cdot 10^3$	$>0.1 \cdot 10^9$	(4)	$>10^8$
2,4,5-Trichlorophenol	6.9**	0.2–0.3	1.2–1.5	*t*-BuOH	3	$<3 \cdot 10^3$	$>1 \cdot 10^9$	(2)	$>10^9$
penta Chlorophenol	4.7**	0.3	2	AcOH	3	$\gg 300 \cdot 10^3$		(1)	$\gg 10^5$
4-Nitrophenol	7.2	0.01–1.4	1.5–3.0	*t*-BuOH	2–7	<50	$16 \pm 5 \cdot 10^6$	(20)	$14 \cdot 10^6$
2-Cresol	10.2	0.01–0.1	1.5/2.0	*t*-BuOH	7	$12 \pm 3 \cdot 10^3$		(6)	
3-Cresol	10.0	$4 \cdot 10^{-3}$	1.5/2.0	*t*-BuOH	7	$13 \pm 3 \cdot 10^3$		(2)	
4-Cresol	10.2	0.01	1.5/2.0	*t*-BuOH	7	$30 \pm 6 \cdot 10^3$		(2)	
Salicylate ion	13.4‖	$(0.03–1)10^{-2}$	3–7	*t*-BuOH	4	$30 \pm 10 \cdot 10^3$		(13)	$<300 \cdot 10^3$
Salicylic acid	3.0/13.4‖	$0.1–1 \cdot 10^2$	1.2	*t*-BuOH	4	<500			
Resorcinol	9.8	0.003	2			$\gg 300 \cdot 10^3$		(1)	$\gg 300 \cdot 10^3$

†See Table 1.
¶All measurements by the indigo method.
‖pK_{HB} of phenolic group.
**pK_{HB} values from own measurements performed with same buffers and pH calibrations as those used for kinetic experiments. Method: The conc. of B^-/HB was measured by u.v. absorption vs pH (multicomponent method).

7. Methods of estimation of reaction rate coefficients in ozonation

7.1. Competitive kinetic model

A competitive kinetic model was proposed by Gurol and Negouniaini (1984). In this method, mixtures of organic compounds are degraded simultaneously in a reaction system. In every mixture, one of the organic substances is a reference compound, which degradation rate constant is previously known. The remaining substances constitute the target compounds, whose rate constants are unknown. This dynamic approach has been used with success by several authors (Hoigné and Bader, 1983, Benitez et al., 1998, Yao and Haag, 1991) This procedure is reliable when measuring the rates of fast reactions in aqueous solutions, and is based on assuming that the reaction between the oxidant and the organic follows second order kinetics, that is, first order with respect to both reactants.
In a specific case of ozonation of chlorophenol mixtures (Benitez et al., 2000), the rate expression of disappearance for each chlorophenol CP_i and the reference chlorophenol CP_R is

$$-\frac{d[CP_i]}{dt} = k_i[O_3][CP_i] = \frac{k_{O_3 i}}{\gamma_i}[O_3][CP_i] \qquad (7.1)$$

$$-\frac{[CP_R]}{dt} = k_R[O_3][CP_R] = \frac{k_{O_3 R}}{\gamma_R}[O_3][CP_R] \qquad (7.2)$$

where $k_{O_3 R}$ and $k_{O_3 i}$ are the overall ozone disappearance rate constants for the reference and target compounds. k_R and k_i are the overall CP disappearance rate constants for the reference and target compounds. γ_R and γ_i are the stoichiometric ratios for the reference and the target compound, respectively.
By integrating equations 7.1 and 7.2 between $t = 0$ and $t = t$, and dividing the obtained equations the following equation is obtained

$$\ln\frac{[CP_i]_0}{[CP_i]} = \frac{\gamma_R k_{O_3 i}}{\gamma_i k_{O_3 R}} \ln\frac{[CP_R]_0}{CP_R} \qquad (7.3)$$

In this method the stoichiometric coefficients have to be known to obtain $k_{O_3 i}$. A plot of $\ln\frac{[CP_i]_0}{[CP_i]}$ against $\ln\frac{[CP_R]_0}{[CP_R]}$ must yield a straight line whose slope is the ratio of the rate constants.

7.1.1 Calculation of overall reaction rate coefficient from reaction rates of anionic and neutral forms of solute

An acidic component dissociates in a water solution according to Equation 7.4. If the reaction rate coefficients of the anionic and neutral forms of the dissociated component M are known, the overall reaction rate coefficient can be calculated from α, the degree of dissociation, defined as

$$\alpha = \frac{[M^-]}{[M^- + M]} \qquad (7.4)$$

On the other hand, the degree of dissociation can also be determined from the pH of the solution and the dissociation constant K_a of the acid

$$\alpha = \frac{1}{1 + \frac{[H^+]}{K_a}} \qquad (7.5)$$

The disappearance rate of ozone can be written as

$$r_{O_3} = k_{O_3}[O_3][M]_{tot} = k_{O_3 M^-}[O_3][M^-] + k_{O_3 M}[O_3][M] \qquad (7.6)$$

From Equations 7.4 and 7.6 it can be stated that

$$k_{O_3} = \alpha k_{O_3, M^-} + (1-\alpha) k_{O_3, M} \qquad (7.7)$$

Where k_{O_3} is the overall reaction rate coefficient of ozone decomposition and $k_{O_3M^-}$ and k_{O_3M} are the reaction rate coefficients of ozone decomposition in ozone reactions with M^- and M, respectively.

7.1.2 Determination of the stoichiometric coefficients

In literature, the stoichiometric coefficients in ozonation are usually determined from the decomposed amounts of ozone and solute during the initial phase of ozonation in a well mixed reactor. In literature, the initial phase is usually a few minutes of reaction time.
The decomposition rate of solute M can expressed

$$-\frac{d[M]}{dt} = k[O_3][M] \qquad (7.8)$$

The ozone decomposition rate can be expressed with

$$-\frac{d[O_3]}{dt} = \gamma k[O_3][M] \qquad (7.9)$$

where $$\gamma = \frac{[O_3]_0 - [O_3]}{[M]_0 - [M]} \qquad (7.10)$$

When using this method it has to be supposed that the amount of moles of intermediate compounds remains relatively small compared with the amount of moles of M and the reactions of the intermediates competing for ozone are sufficiently slow.

7.2 Determination of second order reaction rate coefficient of ozone with an excess of solute component

The rate of ozone disappearance in a batch reaction with solute M with initial concentration $[M]_0$ is

$$-\frac{d[O_3]}{dt} = k_{O_3}[O_3][M] \qquad (7.11)$$

If the concentration of component M is many times higher than that of ozone $[M] \approx [M]_0$ and integration of Equation 7.11 yields

$$\ln\frac{[O_3]}{[O_3]_0} = k_{O_3}[M]_0 t \qquad (7.12)$$

Plotting $\ln([O_3]/[O_3]_0)$ versus time, experimental points should be situated around a straight line with slope equal to $k_{O_3}[M]_0$.
However, batch measurements with several different initial concentrations of ozone and solute should be done to obtain the rate constant applicable to a larger concentration range.

7.3 Estimation of the rate coefficient in the pseudo m-order regime (Benitez et al. 1999)

The pseudo m-order regime of absorption is accomplished when the condition

$$3 < Ha < \frac{E_i}{2} \qquad (7.13)$$

is fulfilled. E_i is the instantaneous reaction factor defined in film theory (Charpentier, 1981).

$$E_i = 1 + \frac{D_M}{D_A}\frac{\gamma[M]}{[A]^*} \qquad (7.14)$$

Ha, the Hatta number, is

$$Ha = \frac{1}{k_L}\sqrt{\frac{2}{m+1}k_A\, D_A [A]^{*m-1}[M]^n} \qquad (7.15)$$

where A refers to the ozone gas absorbing into the solution. k_A is the rate constant for ozone. According to the film theory the gas absorption rate can be expressed by the following equation:

$$N_A = k_L a[A]^* E \qquad (7.16)$$

If the reactions of the intermediates are negligible as regards ozone consumption one can write:

$$N_A = \gamma\left(-\frac{d[M]}{dt}\right) \qquad (7.17)$$

From Equations 7.17 and 7.18 the following form is obtained

$$E = \frac{\gamma\left(-\frac{d[M]}{dt}\right)}{k_L a[A]^*} \qquad (7.18)$$

In the pseudo m-order regime the film theory proposes that $E = Ha$. Thus with Equations 7.15, 7.16 and 7.17 can be written

$$-\frac{d[M]}{dt} = \frac{a[A]^*}{\gamma}\sqrt{\frac{2k_A D_A [A]^{*m-1}[M]^n}{m+1}} \qquad (7.19)$$

Assuming n=1, which is a common situation for ozone-organics reactions, rearranging and integrating with the initial condition

$$t = 0 \qquad [M] = [M]_0 \qquad (7.20)$$

yields

$$[M]_0^{1/2} - [M]^{1/2} = \kappa t \qquad (7.21)$$

where

$$\kappa = \frac{a[A]^*}{2\gamma}\sqrt{\frac{2k_A D_A [A]^{*m-1}}{m+1}} \qquad (7.22)$$

Based on Equation 7.21, a plot of $[M]_0^{1/2} - [M]^{1/2}$ versus reaction time should give a straight line whose slope is κ.
Equation 7.22 allows one to determine the reaction order m for the absorbing and reacting gas A by double plotting κ versus $[A]^*$ with different partial pressures of A. This should yield a straight line with a slope of $(m+1)/2$. Knowing the m value k_A can be calculated from Equation 7.22.

7.4 Estimation of the pseudo first order reaction rate coefficient with an excess of ozone in the solution

When the ozone decomposition rate in solution is low enough, the different steady state concentrations of ozone can be achieved with different gas flow rates in the reactor. In this case, the ozone consumption rate can be determined by the rate of chemical reaction in the bulk solution.(Charpentier, 1981).
Since the oxidizing ability of ozone comes from either molecular ozone or from hydroxyl radicals, the rate of the disappearance of the organic solute can be formulated as follows:

$$-\frac{[M]}{dt} = k_{O_3}[O_3][M] + k_{OH}[OH^-][M] \qquad (7.23)$$

In equation 7.23 k_{O_3} and k_{OH} are the rate coefficients for solute M decomposition. In the steady state situation it can be supposed

that the ozone concentration and hydroxyl radical concentration are constants in the solution. Therefore, Equation 7.23 can be rearranged to the pseudo first-order reaction equation:

$$\frac{d[M]}{dt} = -\left(k_{O_3}[O_3] + k_{OH}[OH^-]\right)[M] = -k[M] \qquad (7.24)$$

When $\ln([M]/[M]_0)$ values are plotted against time the pseudo first-order rate constant is obtained from the slope.

7.5 Quantification of the oxidation of micropollutants by ozone and by OH radicals.

To quantify the extent of oxidation during an ozonation process, it is necessary to combine the characterization of the ozonation process with the available kinetic information. The oxidation of a micropollutant M during an ozonation process can be formulated as follows:

$$-\frac{d[M]}{dt} = k_1[M][O_3] + k_2[M][OH^\bullet] \qquad (7.25)$$

The ratio R_c of the concentrations of OH radicals and ozone can be measured by adding an ozone-resistant probe compound (e.g, *para*-chlorobenzoic acid):

$$R_c = \frac{[OH^\bullet]}{[O_3]} \qquad (7.26)$$

Inserting equation 7.26 in equation 7.25 yields

$$-\frac{d[M]}{dt} = (k_1 + k_2 R_c)[M][O_3] \qquad (7.27)$$

Integration of equation 7.27 for a batch or plug-flow reactor yields:

$$\ln\left(\frac{[M]}{[M]_0}\right) = -(k_1 + k_2 R_c)\int [O_3]dt \qquad (7.28)$$

The fraction f_{OH} of M reacting with OH radicals can be calculated as (von Gunten, 2003)

$$f_{OH} = \frac{k_2 R_c}{k_1 + k_2 R_c} \qquad (7.29)$$

The rate coefficient k_1 can be estimated using radical scavenger like *tert*-butyl alcohol in the ozonation of M. k_2 can be estimated using excess of ozone resistant probe compound like *para*-chlorobenzoic acid in reaction solution.

8. Multicomponent reaction models in ozonation

The intermediates of ozone-organic species reactions are quite well known in some cases (phenols for example) but the reaction schemes and, in particular the reaction rate coefficients in the reaction schemes are poorly known. The measurements of rate coefficients presented in literature are usually done for an individual chemical species. Application of these separate rate coefficients into multicomponent mixture models does not necessarily lead to realistic simulations because various effects influencing the rate coefficients of the reactions between the components are not sufficiently taken into consideration.
One way of building a scheme of a multicomponent reaction model is the application of the radical chain model.

8.1. Radical chain models

Radical chain models consist of a variety of reactions which could be; initiation reactions, propagation reactions, promotion reactions, reversible reactions and scavenging reactions. Unlike the case of irreversible reactions, where only one kinetic rate constant is required to describe the rates of formation and destruction of various species, in the case of reversible reactions, rates for both the forward and backward reactions are needed and may not be available because such reactions are generally described by an equilibrium constant which is the ratio of the forward and backward reaction rates. If the equilibrium presumption is adopted, one must choose the constant in such an arbitrary manner that their ratio is constant. Care must, however, be taken that the rate coefficients are at least an order higher than the largest irreversible rate constant.

8.1.1 Ozonation model for organic species

The model adopted by Rivas et al.(2006) to simulate the ozonation consisted of the classic radical chain mechanism introduced by Hoigné, Staehelin and Bühler (Chelkowska et al., 1992) and fluorene reactions between ozone and hydroxyl radical. Ozone mass transfer was also included in the model. The main reactions constituting the mechanism are as follows. [Units are $mol/\left(dm^3 s\right)$ or $1/s$]

$$O_3 + OH^- \longrightarrow HO^\bullet + {}^\bullet O_2^- \qquad k = 140/70 \qquad (8.1)$$

$$O_3 + {}^\bullet O_2^- \longrightarrow O_2 + {}^\bullet O_3^- \qquad k = 1.6\times 10^9 \qquad (8.2)$$

$$H^+ + {}^\bullet O_3^- \longleftrightarrow HO_3^\bullet \qquad k = 2.0\times 10^{10},\quad k^- = 3.7\times 10^4 \qquad (8.3)$$

$HO_3^{\bullet} \longrightarrow O_2 + HO^{\bullet}$ $k = 5.0\times10^{4}$ (8.4)

$O_3 + HO^{\bullet} \longleftrightarrow HO_4^{\bullet}$ $k = 2.0\times10^{9}, \quad k^{-} = 1.0\times10^{2}$ (8.5)

$HO_4^{\bullet} \longrightarrow O_2 + HO_2^{\bullet}$ $k = 2.8\times10^{4}$ (8.6)

$HO_2^{\bullet} \longrightarrow O_2 + O_3 \quad (+H_2O)$ $k = 1.0\times10^{10}$ (8.7)

$HO^{\bullet} + HO^{\bullet} \longrightarrow H_2O_2$ $k = 5.0\times10^{9}$ (8.8)

$HO^{\bullet} + HO_3^{\bullet} \longrightarrow O_2 + H_2O_2$ $k = 5.0\times10^{9}$ (8.9)

$HO_3^{\bullet} + {}^{\bullet}O_2^{-} \longrightarrow 2O_2 + OH^{-}$ $k = 1.0\times10^{10}$ (8.10)

$HO_4^{\bullet} + HO_4^{\bullet} \longrightarrow 2O_3 + H_2O_2$ $k = 5.0\times10^{9}$ (8.11)

$HO_4^{\bullet} + HO^{\bullet} \longrightarrow O_3 + H_2O_2$ $k = 5.0\times10^{9}$ (8.12)

$HO_4^{\bullet} + {}^{\bullet}O_2^{-} \longrightarrow O_3 + O_2 + OH^{-}$ $k = 1.0\times10^{10}$ (8.13)

$HO_4^{\bullet} + HO_3^{\bullet} \longrightarrow O_3 + O_2 + H_2O_2$ $k = 5.0\times10^{9}$ (8.14)

$(H_2O) + {}^{\bullet}O_3^{-} \longleftrightarrow HO_3^{\bullet} + OH^{-}$ $k = 54.2, \quad k^{-} = 1.0\times10^{10}$ (8.15)

$HO_2^{-} + O_3 \longrightarrow HO^{\bullet} + {}^{\bullet}O_2^{-} + O_2$ $k = 2.8\times10^{6}$ (8.16)

$HO_2^{\bullet} \longleftrightarrow H^{+} + {}^{\bullet}O_2^{-}$ $k = 3.2\times10^{5}, \quad k^{-} = 2.0\times10^{10}$ (8.17)

$H_2O_2 \longleftrightarrow H^{+} + HO_2^{-}$ $k = 4.5\times10^{-2}, \quad k^{-} = 2.0\times10^{10}$ (8.18)

$H^{+} + OH^{-} \longleftrightarrow H_2O$ $k = 1.0\times10^{11}, \quad k^{-} = 1.0\times10^{-3}$ (8.19)

$$O_3 + F \longrightarrow P \qquad k_{O_3-F} \qquad (8.20)$$

$$HO^{\bullet} + F \longrightarrow P \qquad k_{HO^{\bullet}-F} \qquad (8.21)$$

F is fluorene and P denotes products. Rivas et al. found in their investigation that the ozone reactions with intermediate products from ozone-fluorene reactions cannot be ignored. Taking the intermediates reactions with ozone and hydroxyl radicals into the model, they obtained better simulation results for ozone gas leaving the reactor and for dissolved ozone.

8.1.2 Ozone reactions in pure water containing bicarbonate/carbonate alkanity

Kumar and Bose (2004) presented a model for ozone decomposition taking into consideration the scavenging effect of inorganic carbon. Their reaction model which is based on the Hoigné-Staehelin-Bader model(HSB)is as follows:

Initiation reactions

$$O_3 + OH^- \longrightarrow {}^{\bullet}O_2^- + HO_2^{\bullet} \qquad k = 70\,dm^3/(mol\,s) \qquad (8.22)$$

$$O_3 + HO_2^- \longrightarrow {}^{\bullet}O_3^- + HO_2^{\bullet} \qquad k = 5.5\times10^6\,dm^3/(mol\,s) \qquad (8.23)$$

Propagation reactions

$$O_3 + {}^{\bullet}O_2^- \longrightarrow O_3^- + O_2 \qquad k = 1.6\times10^9\,dm^3/(mol\,s) \qquad (8.24)$$

$$H^+ + {}^{\bullet}O_3^- \longrightarrow {}^{\bullet}HO_3 \qquad k = 5.2\times10^{10}\,dm^3/(mol\,s) \qquad (8.25)$$

$$^{\bullet}HO_3 \longrightarrow OH + O_2 \qquad k = 1.1\times10^5\,dm^3/(mol\,s) \qquad (8.26)$$

Promotion reactions

$$O_3 + {}^{\bullet}OH \longrightarrow {}^{\bullet}HO_2 + O_2 \qquad k = 1.1\times10^{8}\ dm^3/(mol\,s) \qquad (8.27)$$

$$H_2O_2 + {}^{\bullet}OH \longrightarrow {}^{\bullet}HO_2 + H_2O \qquad k = 2.7\times10^{7}\ dm^3/(mol\,s) \qquad (8.28)$$

$$HO_2^- + {}^{\bullet}OH \longrightarrow {}^{\bullet}O_2^- + H_2O \qquad k = 7.5\times10^{9}\ dm^3/(mol\,s) \qquad (8.29)$$

$${}^{\bullet}HO_2 + {}^{\bullet}OH \longrightarrow H_2O + O_2 \qquad k = 1.0\times10^{10}\ dm^3/(mol\,s) \qquad (8.30)$$

Formation of H_2O_2

$${}^{\bullet}HO_2 + {}^{\bullet}HO_2 \longrightarrow H_2O_2 + O_2 \qquad k = 8.3\times10^{5}\ dm^3/(mol\,s) \qquad (8.31)$$

$$H_2O + {}^{\bullet}HO_2 + {}^{\bullet}O_2^- \longrightarrow H_2O_2 + O_2 + OH^- \qquad k = 9.7\times10^{7}\ dm^3/(mol\,s) \qquad (8.32)$$

Reversible reactions

$${}^{\bullet}HO_2 \longleftrightarrow H^+ + {}^{\bullet}O_2^- \qquad k/k^- = 10^{-4.8} \qquad (8.33$$

$$H_2O_2 \longleftrightarrow HO_2^- + H^+ \qquad k/k^- = 10^{-11.8} \qquad (8.34)$$

$$H_2O \longleftrightarrow OH^- + H^+ \qquad k/k^- = 10^{-14} \qquad (8.35)$$

$$H_2CO_3 \longleftrightarrow HCO_3^- + H^+ \qquad k/k^- = 10^{-6.3} \qquad (8.36)$$

$$HCO_3^- \longleftrightarrow CO_3^{2-} + H^+ \qquad k/k^- = 10^{-10.3} \qquad (8.37)$$

Scavenging reactions

$$HCO_3^- + {}^{\bullet}OH \longrightarrow {}^{\bullet}CO_3^- + H_2O \qquad k = 1.1\times10^{7}\ dm^3/(mol\,s) \qquad (8.38)$$

$$CO_3^- + {}^{\bullet}OH \longrightarrow {}^{\bullet}CO_3^- + OH^- \qquad k = 4.0\times10^{8}\ dm^3/(mol\,s) \qquad (8.39)$$

$$^{\bullet}CO_3^- + {}^{\bullet}OH \longrightarrow {}^{\bullet}CO_3^- OH^- \qquad k = 3.0\times10^9\ dm^3/(mol\,s) \qquad (8.40)$$

Using their reaction model, Kumar and Bose made simulations at various pH and at various radical scavenger concentrations rather successfully.

8.1.3 Ozone reactions in pure water containing bicarbonate/carbonate alkanity and the organics

Pedit et al. (1997) presented a model with ozone decomposition chemistry including degradation of TCE and PDE, carbon as a scavenger, and other reversible reactions. Their reactions are as follows:

Initial reactions

$$HO_2^- + O_3 \longrightarrow {}^{\bullet}O_3^- + HO_2^{\bullet} \qquad k = 5.5\times10^6\ dm^3/(mol\,s) \qquad (8.41)$$

$$OH^- + O_3 \longrightarrow HO_2^- + O_2 \qquad k = 70\ dm^3/(mol\,s) \qquad (8.42)$$

Propagation reactions

$$^{\bullet}O_2^- + O_3 \longrightarrow {}^{\bullet}O_3^- + O_2 \qquad k = 1.6\times10^9\ dm^3/(mol\,s) \qquad (8.43)$$

$$^{\bullet}O_3^- + H^+ \longrightarrow HO_3^{\bullet} \qquad k = 5.2\times10^{10}\ dm^3/(mol\,s) \qquad (8.44)$$

$$HO_3^{\bullet} \longrightarrow OH^{\bullet} + O_2 \qquad k = 1.1\times10^5\ 1/s \qquad (8.45)$$

Destruction and scavenging reactions

$$O_3 + TCE \longrightarrow products \qquad k = 17\ dm^3/(mol\,s) \qquad (8.46)$$

$$O_3 + PCE \longrightarrow products \qquad k = 0.1\,dm^3/(mol\,s) \qquad (8.47)$$

$$OH^{\bullet} + TCE \longrightarrow products \qquad k = 4.0\times10^{9}\ dm^{3}/(mol\,s) \qquad (8.48)$$

$$OH^{\bullet} + PCE \longrightarrow products \qquad k = 2.0\times10^{9}\ dm^{3}/(mol\,s) \qquad (8.49)$$

$$OH^{\bullet} + HO_2^{-} \longrightarrow OH^{-} + HO_2^{\bullet} \qquad k = 7.5\times10^{9}\ dm^{3}/(mol\,s) \qquad (8.50)$$

$$OH^{\bullet} + H_2O_2 \longrightarrow H_2O + HO_2^{\bullet} \qquad k = 2.7\times10^{7}\ dm^{3}/(mol\,s) \qquad (8.51)$$

$$OH^{\bullet} + HCO_3^{-} \longrightarrow H_2O + {}^{\bullet}CO_3^{-} \qquad k = 8.5\times10^{6}\ dm^{3}/(mol\,s) \qquad (8.52)$$

$$OH^{\bullet} + CO_3^{2-} \longrightarrow OH^{-} + {}^{\bullet}CO_3^{-} \qquad k = 3.9\times10^{8}\ dm^{3}/(mol\,s) \qquad (8.53)$$

$$OH^{\bullet} + O_3 \longrightarrow HO_2^{\bullet} + O_2 \qquad k = 1.1\times10^{8}\ dm^{3}/(mol\,s) \qquad (8.54)$$

$${}^{\bullet}CO_3^{-} + H_2O_2 \longrightarrow HO_2^{\bullet} + HCO_3^{-} \qquad k = 8.0\times10^{5}\ dm^{3}/(mol\,s) \qquad (8.55)$$

$${}^{\bullet}CO_3^{-} + HO_2^{-} \longrightarrow {}^{\bullet}O_2^{-} + HCO_3^{-} \qquad k = 5.6\times10^{7}\ dm^{3}/(mol\,s) \qquad (8.56)$$

$$HO_2^{\bullet} + HO_2^{\bullet} \longrightarrow O_2 + H_2O_2 \qquad k = 8.3\times10^{5}\ dm^{3}/(mol\,s) \qquad (8.57)$$

$${}^{\bullet}O_2^{-} + HO_2^{\bullet} + H_2O \longrightarrow O_2 + H_2O_2 + OH^{-} \qquad k = 9.7\times10^{7}\ dm^{3}/(mol\,s) \qquad (8.58)$$

$${}^{\bullet}CO_3^{-} + {}^{\bullet}CO_3^{-} \longrightarrow products \qquad k = 2.2\times10^{6}\ dm^{3}/(mol\,s) \qquad (8.59)$$

Equilibrium reactions

$$H_2O_2 \longleftrightarrow HO_2^{-} + H^{+} \qquad pK = 11.7 \qquad (8.60)$$

$$HO_2^{\bullet} \longleftrightarrow {}^{\bullet}O_2^{-} + H^{+} \qquad pK = 4.8 \qquad (8.61)$$

$$H_2CO_3 \longleftrightarrow HCO_3^- + H^+ \qquad pK = 6.3 \qquad (8.62)$$

$$H_2O \longleftrightarrow OH^- + H^+ \qquad pK = 14 \qquad (8.63)$$

8.2 Multicomponent reaction models without radical chain reactions and reduction in the number of model parameters

During oxidation of organics a large number of various intermediates are usually produced. In addition, a large number of oxidation species are also produced, for example radicals. A natural choice for deal with the reaction system is a development of a reaction model where COD has an important role in presenting the unknown (and in some cases known) intermediates. In some special cases, however, sum parameters are needed because of some oxidation intermediates that cannot be presented as COD.

8.2.1 Model of apparent rate coefficients

When organics A and B react with ozone producing known or unknown byproducts C and D, one can write

$$A + O_3 \xrightarrow{k_1} C \qquad (8.64)$$

$$B + O_3 \xrightarrow{k_2} D \qquad (8.65)$$

If one writes differential equations to solve the concentrations directly according to equations 8.64 and 8.65, one obtains apparent rate coefficients k_1 and k_2 because the stoichiometric

coefficients for ozone have been neglected. The model itself is fully empirical.

8.2.2 Model neglecting ozone consumption of intermediates

Suppose that the stoichiometric coefficients for ozone γ_1 and γ_2 are known. When organics A and B react with ozone producing unknown by-products C and D one can write

$$A + \gamma_1 O_3 \xrightarrow{k_1} C \qquad (8.66)$$

$$B + \gamma_2 O_3 \xrightarrow{k_2} D \qquad (8.67)$$

C and D can be renamed as (unknown) products without including them in the differential equations. In this case it is supposed that the ozone consumption of the products is negligible compared to reactants A and B.

8.2.3 Residual COD model

A natural choice to include the unknown (and known) intermediates in the reaction model is the use of residual COD as a lumped parameter. COD_{res} represents the COD of the intermediate species which is the measured total COD from which the theoretical COD of the measured intermediates has been subtracted. This model has been used in estimation of the reaction kinetics in this thesis.
Suppose that the rate coefficients and the stoichiometric coefficients of a ozonation raction system with reactants A, B and known intermediate species C has to be estimated.

$$A + \gamma_1 O_3 \xrightarrow{k_1} C + \gamma_2 COD_{res} \qquad (8.68)$$

$$B + \gamma_3 O_3 \xrightarrow{k_2} \gamma_4 COD_{res} \qquad (8.69$$

$$C + \gamma_5 O_3 \xrightarrow{k_3} \gamma_6 COD_{res} \qquad (8.70)$$

$$COD_{res} + \gamma_7 O_3 \xrightarrow{k_4} CO_2 + H_2O \qquad (8.71)$$

The stoichiometric coefficient $\gamma_7 = 2/3$ can be easily calculated from the stoichiometric need of ozone to oxidate 1 mole COD_{res}.

Reaction model equations have to be written in differential form for the nonlinear parameter estimation of rate coefficients $k_1 - k_5$ and the stoichiometric coefficients $\gamma_1 - \gamma_6$.

$$r_i = -\frac{d[i]}{dt} = \sum_{i \neq O_3} k_i \gamma_i [O_3][i] \qquad (8.72)$$

$$\frac{d[A]}{dt} = -k_1[A][O_3] \quad \frac{d[B]}{dt} = -k_2[B][O_3] \quad \frac{d[C]}{dt} = -k_3[C][O_3] \qquad (8.73)$$

$$\frac{d[O_3]}{dt} = -k_1\gamma_1[A][O_3] - k_2\gamma_3[B][O_3] - k_3\gamma_5[C][O_3] - k_4[COD_{res}][O_3] \qquad (8.74)$$

$$\frac{d[COD_{res}]}{dt} = k_1\gamma_3[A][O_3] + k_2\gamma_4[B][O_3] + k_3\gamma_6[C][O_3] - k_4\frac{3}{2}[COD_{res}][O_3] \qquad (8.75)$$

In the above, there are three COD_{res} producing equations (Equations 8.68–8.70). The number of estimable parameters is ten. In equation 8.71 it is presumed that the reduction of COD_{res} consumes a stoichiometric amount of O_3. However, if one writes equation 8.71 as

$$COD_{res} + \gamma_7 O_3 \xrightarrow{k_4} CO_2 + H_2O \qquad (8.71\ b)$$

the number of estimable parameters is eleven. And equation 8.75 becomes:

$$\frac{d[COD_{res}]}{dt} = k_1\gamma_3[A][O_3] + k_2\gamma_4[B][O_3] + k_3\gamma_6[C][O_3] - k_4\gamma_7\frac{3}{2}[COD_{res}][O_3] \qquad (8.75\ b)$$

It can be determined that the number of estimable parameters is at least equal to *three times the number of* COD_{res} *production equations + 1.*

In the case of a multireaction model, the model presented above produces a large number of estimable parameters. In nonlinear parameter estimation the danger of over parametrization is immense.

8.2.4 Residual COD model with theoretical COD values of the reacting compounds

The ozone reactions with A and B can be written as

$$A + \gamma_i O_3 \rightarrow P \qquad (8.76)$$

$$B + \gamma_j O_3 \rightarrow P \qquad (8.77)$$

where P represents the known and the unknown intermediates with a degree of oxidation determined by the stoichiometric coefficients γ_i and γ_j. The reactions 8.76 and 8.77 can also be expressed through COD using the theoretical oxygen consumptions for A and B calculated from their molecular structure and the residual COD calculated on the principle explained earlier. Using this approach, the complete reaction model can be presented as

$$A + \gamma_1 O_3 \xrightarrow{k_1} C + COD_{res} \qquad (8.78)$$

$$B + \gamma_2 O_3 \xrightarrow{k_2} COD_{res} \qquad (8.79)$$

$$C + \gamma_3 O_3 \xrightarrow{k_3} COD_{res} \qquad (8.80)$$

$$COD_{res} + \frac{2}{3}O_3 \xrightarrow{k_4} CO_2 + H_2O \qquad (8.81)$$

γ_i is the stoichiometric coefficient for ozone. In the reaction rate equations, the stoichiometric coefficients γ_A, γ_B and γ_C are the theoretical oxygen demands for A, B and C. With this procedure, equations 8.78–8.80 can be written as reaction equations for the COD and ozone. The COD_{res} produced in equations 8.78–8.80 can be written as $(\gamma_A - \gamma_1\ 3/2\ )A$ and $(\gamma_B - \gamma_2\ 3/2\ )B$ and $(\gamma_C - \gamma_3\ 3/2\ )C$ can be found in equation 8.84. $\gamma_1\ 3/2$ represents the theoretical COD reduction by γ_1 moles of O_3.
The reaction rate equations 8.82–8.84 are written in the mode of equation (8.72):

$$r_A = -\frac{d[A]}{dt} = k_1[O_3][A] \qquad r_B = -\frac{d[B]}{dt} = k_2[O_3][B] \qquad r_C = -\frac{d[C]}{dt} = k_3[O_3][C] \quad (8.82)$$

$$r_{O_3} = -\frac{d[O_3]}{dt} = k_1\gamma_1[O_3][A] + k_2\gamma_2[O_3][B] + k_3\gamma_3[O_3][C] + k_4[COD][O_3] \qquad (8.83)$$

$$r_{COD_{res}} = -\frac{d[COD_{RES}]}{dt} = -k_1(\gamma_A - \gamma_1\frac{3}{2})[O_3][A] - k_2(\gamma_B - \gamma_2\frac{3}{2})[O_3][B] - k_3(\gamma_C - \gamma_3\frac{3}{2})[O_3][C] +$$

$$k_4\frac{3}{2}[O_3][COD_{res}] \qquad (8.84)$$

The reaction equations 8.78–8.81, written for the reactions between ozone and the solutes, represent ozone decomposition reactions giving reaction products such that the amount of consumed oxygen calculated from the ozone depletion is according to the stoichiometry needed to oxidize each reactant to products. In some particular reactions and circumstances, the theoretical stoichiometry $COD:O_2$ calculated from the reacting ozone could be 1:1 (Beltrán et al., 2000). However, in reaction schemes involving complex radical chain reactions this seems not to be the case. In this research it was found to be necessary to include an additional ozone self-decomposition reaction term in p-nitrophenol

ozonation with initial pH 5 (Appendix III, equation 18, rate coefficient k_5) in the model so that all the ozone consumed in the experiments could be consumed also in the model(Appendix III).

From the number of equations 8.78–8.81 and the number of estimable parameters in them one can determine that the number of estimable parameters is at least equal to *two times the number of* COD_{res} *production equations + 1.*

Compared to the COD_{res} method in paragraph 8.2.3 such a developed method may give a radical decrease in the number of estimable parameters in ozonation of multicomponent reaction systems.

8.2.5. Further actions to decrease the number of estimable model parameters

The straight forward method for decreasing the number of the oxidation reaction model parameters is to write the reaction system equations according to fulfillment of the stoichiometric need of theoretical O_2. The consumption of O_3 of the reaction can be calculated from this theoretical O_2. However in literature ozonation reaction systems written with this procedure are surprisingly rare if the radical chain reactions are not considered.

In many cases it is possible to compute the need of O_3 to oxidize the reacting compound to intermediate compounds produced or to end products produced from the theoretical O_2. In Equation 8.81 the reaction of ozone with COD_{res} producing CO_2 and H_2O was written with the stoichiometric coefficient 2/3 for O_3. Similarly, the oxidation reaction of nitrite to nitrate requires 1/3 moles of O_3, etc. In this research it was shown that it is possible to estimate

multicomponent model parameters, for example, rate coefficients, stoichiometrich coefficients and also $k_L a$ reliably using the kind of approach presented in chapter 12.3.

8.2.6 Comparison of multicomponent reaction kinetic models

Modeling of ozone contactors involves a comprehensive mathematical description of the system. In addition to chemical kinetics physical conditions must to be taken into consideration. The solubility can be represented by a partition coefficient, e.g., Henry's coefficient, and the mass transfer can be calculated with $k_L a$. The hydrodynamics has to be taken into consideration, both below the liquid surface level and in the headspace of the reactor. In tall bubble columns, the change of hydrostatic pressure must be accounted for and also ozone self-decomposition in the tall headspace.

Radical chain models (mechanistic models) have an advantage in that they depict the whole reaction chain accurately without any sum parameters. They are advantageous in simulation of reactors that have sections without good mixing conditions in the liquid phase. That comes from the possibility that some organic component may react preferentially with ozone or hydroxyl radical. The result is concentration deviations with e.g. hydroxyl radical or ozone, which lead to different reaction rates of a component in different parts of the reactor. A radical chain method also offers a direct mechanism to consider the effect of pH and carbon balance. However, if one wants to build a reaction model containing all radical reactions and reactions of inorganic and organic components with both, ozone and hydroxyl radical, a large

amount of analytical work is needed to characterize the waste water. In addition, one has to collect a large amount of reaction kinetic data, rate coefficients and stoichiometric coefficients. Typically, the kinetic data comes from a number of authors who most probably obtained them with different water matrix. The result is that one has a large amount of kinetic data with rate coefficients containing a considerable uncertainty. The sum effect is that the reaction model has a lot of uncertainty in simulation accuracy. The benefit of the residual COD model is that the relatively small number of parameters means fast and reliable estimation of the kinetic parameters needed for a specific ozonation process.

9. Parameter Estimation

9.1. General Theory

During parameter estimation a sensitivity analysis must be conducted to obtain information on reliability and identifiability of the estimated parameters and to avoid ‘false’ parameters that have not particular physical meaning. This is strongly recommended especially in parameter estimation of models with a high number of parameters to be estimated. In this chapter 9 some aspects of general theory of parameter estimation are discussed and illustrated with ozonation parameter estimation results (Appnedix I, II, III and IV).

9.1.1 Physical Model

A mechanistic model can be formally written in the following form (Haario, 1994):

$$s = f(x, \beta, c) \qquad (9.1)$$

$$y_p = g(s) = s\,, \qquad (9.2)$$

where the markings are:

s the state of the system

y_p the observed (response) variable predicted by the model, for example $P_{O_3 o}$ in this study

x the experimental variables, for example $P_{O_3 i}$ and $[O_3]$ or $P_{O_3 i}$, $[O_3]$ and U

β the estimated parameters, for example $k_L a$ and H or B_1, B_2 and H

c constants

Function f describes the model itself, while g gives information on the available observations. In this case, g is equal to state s.

9.1.2 Least Squares Optimization

The closeness of the data and values predicted by the model can be measured, in principle, using several criteria. The most common objective function based on which the parameters are estimated is, however, the sum of the residual squares. If observations $y_i = P_{O_3 o}$ are available at the experimental points ($P_{O_3 i}$, $[O_3]$) or ($P_{O_3 i}$, $[O_3]$, U), (U = velocity), the sum of the squares of the residuals between the model and data is given by

$$l(\beta) = \left\| y - y_p \right\|^2 = \sum_{i=1}^{n} (y_i - y_{ip})^2 \qquad (9.3)$$

where the values of y_{ip} denote the predictions of $P_{O_3 o}$ given by the model with the estimated parameter values, β, and n is the number of observations in the data set. To bring the values of y_p as close to y as possible in the average sense, the above sum is minimized with respect to β.

9.1.3 Sensitivity analysis using an objective function

The aim of parameter estimation is to find correct values for the model parameters. The question of identifiability can be addressed using the objective function, l, the solution point of the least squares problem. By plotting one- or two-dimensional contour lines of l, one can study the identifiability of the problem. If the values of the objective function change rapidly in every direction from the peak point, the parameters are well defined.

Minimization of the objective function, l, can be performed with a number of different optimization routines. In this research, a nonlinear simplex optimization method (Rao, 1998) was used.

The reliability and identifiability of the estimated parameters was studied by plotting one- and two-dimensional contour lines of the objective function l. The length of the interval of the parameter axis can be chosen for example to be five times the estimated standard error of the parameter. In a normal distribution it is interpreted that the parameter value is within a probability of 95 % in range of two standard deviations of the mean. When analyzing the objective function contour plots in Figure 9.1 one can see that the global minimum point is found. This reference point (+) represents the estimated parameter values k_2 and k_3. The true values of these coefficients are to a high degree of probability in the immediate vicinity of the computed minimum, because the value of function l increases relatively rapidly when moving from the minimum in the directions of the parameter axis.

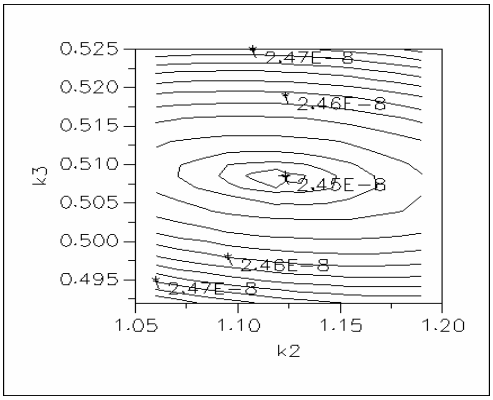

Figure 9.1 Contour plot $l(k_2,k_3)$ of the objective function l

9.1.4 Coefficient of determination

The most common measure of the goodness of fit is the coefficient of determination (the R^2 value). The idea is to compare the residuals, $y-y_p$, given by the model to those of the average value $\bar{y}$ of all the data points. The R^2 value is given by the expression

$$R^2 = 100(1 - \frac{\left\| y - y_p \right\|^2}{\left\| y - \bar{y} \right\|^2}) \%$$ (9.4)

The closer R^2 is to 100 %, the more perfect is the fit.

9.1.5 Sensitivity analysis and Jacobian matrix

One method for parameter estimation is to compute the model's Jacobian matrix, the components of which are the first derivatives of the response variables with respect to the parameters. They are the so-called sensitivity coefficients

$$J_{j,p} = \frac{\partial y_p(x_j, \beta)}{\partial \beta},$$ (9.5)

where β is the estimable. The sensitivity coefficients are important because they indicate the magnitude of change of the response y_p due to perturbations in the values of the parameters.

9.1.6 Approximate correlation matrix

The ij element of the correlation matrix is given by (Beck and Arnold, 1977)

$$r_{ij} = P_{ij}(P_{ii}P_{jj})^{-1/2} \qquad (9.6)$$

with the standard assumptions of uncorrelated and constant variance measurement errors and the standard deviation being unknown, P_{ij} is a term of equation 9.7. The estimated covariance of the ordinary least squares estimator vector for parameters $b_{LS}=(X^TX)^{-1}X^TY$ is given by:

$$\mathbf{COV}(b_{LS}) \approx (X^TX)^{-1}s^2, \qquad (9.7)$$

where $$s \approx ((Y-\hat{Y})^T(Y-\hat{Y}))/(n-p) \qquad (9.8)$$

X is the sensitivity matrix $X = (\nabla_\beta y_p^T)^T$, Y the observation vector and $\hat{Y}$ the predicted vector of the observations. The diagonal elements of matrix r are all unity and the off-diagonal element must be within the interval [1,-1]. Whenever the absolute values of all the off-diagonal elements exceed 0.9 in magnitude, the estimates are highly correlated and tend to be inaccurate.

9.2 MCMC analysis

Traditional regression analysis, as described above, results in a single estimate for the parameter values that give the optimal fit to the measured data in the LSQ (least squares) sense. In addition, estimates about the standard error in the estimates can be produced by linearization of the model. The results of the classical analysis are approximate and possible cross-correlations of the parameters may not be properly revealed. In addition, the reliability is not at all considered in the model predictions.

The question of the identifiability of the parameters (how good and unique our estimate is) and the accuracy of the model predictions can be answered with MCMC (Markov chain Monte Carlo) methods. In this thesis MCMC method was used in analysis of the parameters in the p-nitrophenol ozonation model. In MCMC, the estimation problem is handled in a Bayesian way: the parameters are treated as random variables that have a statistical distribution with many possible values. Instead of a single fit, MCMC analysis determines 'all' parameter values (i.e. a representative sample of their distribution) that give good fits to the data. The size of the measurement error can be estimated with classical statistics using the residuals or it may be sampled as well. For more details, see Gelman et al.,1996 or Solonen,

2006. In this thesis the distribution of the unknown parameters is sought using an effective adaptive MCMC sampling algorithm, introduced by Haario (2001). Typically 20000 – 30000 samples for the unknown parameters were produced. The classical statistical analysis was performed based on linearization on the LSQ optimum. To test and compare the methods, corresponding results were also calculated from the MCMC samples. In addition, statistical error bounds for the model predictions were produced with MCMC.

The sample was used to examine the reliability of the traditional parameter estimation (LSQ fitting) results. The same error and correlation estimates as produced by the classical statistical analysis, based on linearization on the LSQ optimum, were calculated from the MCMC samples. In addition, statistical error bounds for the model predictions were produced with MCMC. In Table 9.1 (see estimable parameters in Appendix III) the standard deviation given by the classical analysis is compared to the values calculated from the MCMC chain. In addition, 95% confidence intervals are given for the parameters, calculated from the MCMC samples. In classical analysis, confidence intervals are formed by linearization and by assuming a distribution for the parameters, whereas in MCMC the confidence interval can be calculated directly from the empirical distribution given by the method, resulting in the more reliable and realistic information about the variation in the estimated parameters.

Table 9.1 Estimated values of k_1 –k_6, γ_1 and γ_2 and standard deviations.

Parameter, dimension	Estimated value	Estimated STD *(relative)*	STD by MCMC	95% interval by MCMC
k_1, $\frac{dm^3}{mol\ s}$	73.4	5.82 *(7.9 %)*	6.53	[65.4 – 91.1]
k_2, $\frac{dm^3}{mol\ s}$	34.3	3.07 *(9.0 %)*	3.29	[29.7 – 42.6]
k_3, $\frac{dm^3}{mol\ s}$	198	16.3 *(8.2 %)*	18.4	[175 – 247]
k_4, $\frac{dm^3}{mol\ s}$	192	42.2 *(9.5 %)*	20.2	[168 – 247]
k_5, $\frac{dm^3}{mol\ s}$	9.63	0.68 *(7.1 %)*	0.73	[8.40 – 11.3]
k_6, $\frac{dm^3}{mol\ s}$	1.71	0.30 *(17.8 %)*	0.32	[1.15 – 2.42]
γ_1	3.03	0.19 *(6.4 %)*	0.20	[2.62 – 3.42]
γ_2	0.2×10^{-8}	1.6×10^{-5} *(8030 %)*	0.047	[0.00 – 0.17]

The results of the MCMC analysis of p-nitrophenol ozonation with initial pH 5 for the reaction rate coefficients k_1 – k_5 are presented in Fig. 9.2 (the estimable parameters are explaned in Appendix III.) The analysis shows that the parameters are well-identified: the distributions are centered on the most probable point, which is close to the point received from the nonlinear LSQ fitting. The correlations given by the correlation matrix in Table 9.1 are also revealed by MCMC: they can be read from the direction and shape of the two-dimensional distributions.

The MCMC analysis for stoichiometric coefficients γ_1 and γ_2 is presented in Fig. 9.3, from which one can see that γ_2 stays very close to zero. The MCMC method gives a larger standard deviation and confidence interval for γ_2 than the classical analysis. Furhermore the correlation information related to γ_1 given by the classical analysis differs from the values calculated from the MCMC sample (see Table 9.1). The analysis shows that γ_2 is poorly identified and all small enough values seem to produce good enough fits.

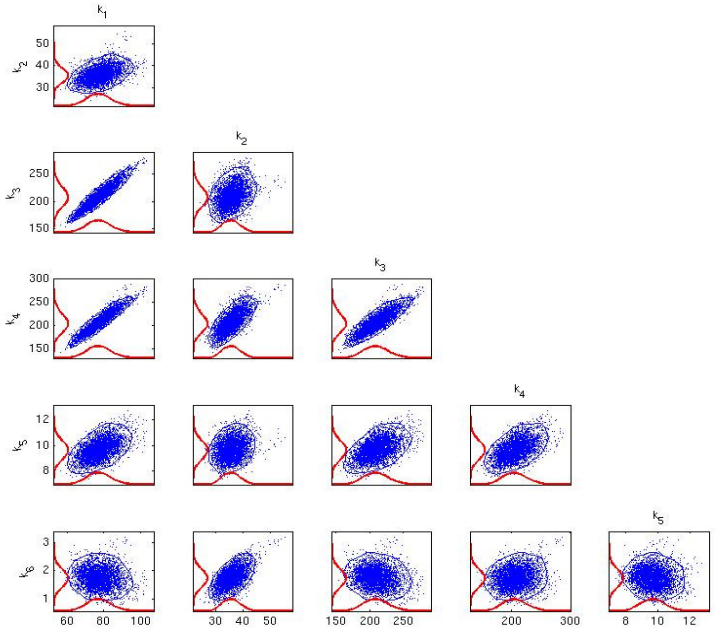

Figure 9.2 MCMC analysis for the reaction rate coefficients. The distribution of the parameters is plotted for each parameter and parameter pair. The outer line represents the 95% confidence region.

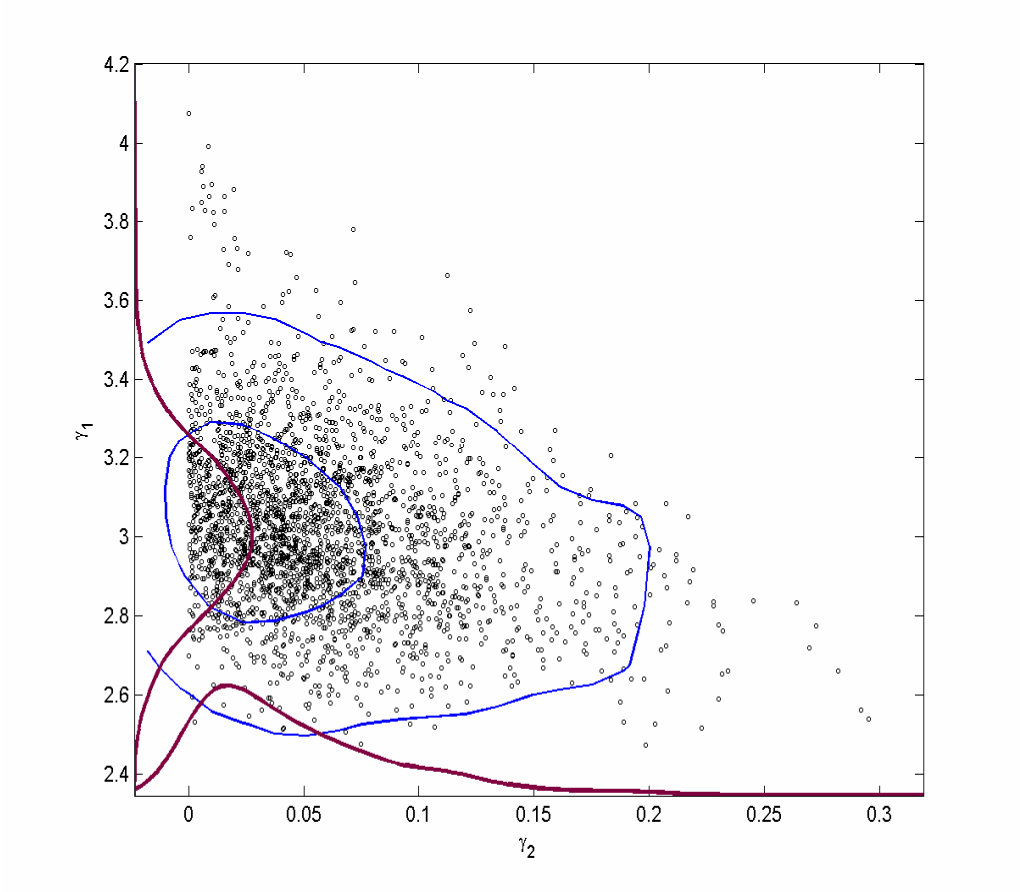

Figure 9.3 MCMC analysis for the stoichiometric coefficients γ_1 and γ_2.

The MCMC analysis can be extended to describe the uncertainties in the model responses (concentrations). This is done by calculating the predictions given by the different sampled parameter values, and plotting selected confidence limits for the predictions at given time points. This type of analysis is shown in Appendix III,

in Figure 8 for p-nitrophenol, in Figure 9 for hydroquinone, in Figure 10 for a nitrate ion, and in Figure 11 for the COD. The analysis shows that the p-nitrophenol concentration is fitted accurately, but the other model components contain more uncertainty. Only one experiment is plotted for each component, because the distribution is rather similar in the other runs.

The darker gray areas in the plots are produced simply by calculating the response components with the parameter values given by the MCMC run. Thus, the darker gray area gives a distribution for the model response. The lighter gray area represents the model predictions with added measurement noise. It means, roughly speaking, the area from which observations (present and ones yet to come) can be expected to be found with certain probability. Thus, the lighter gray area estimates the combined uncertainty of model predictions and measurements. The solid line represents the median of the model predictions.

Markov Chain Monte Carlo (MCMC) -methods can be used to find, instead of single least squares estimates, ‘all’ parameter values with which the model fits to the measured data with the accuracy of the measurement error. The MCMC analysis was useful in getting qualitative and quantitative information about the accuracy and reliability of parameter estimation. In the cases studied during the research for this thesis the MCMC analysis revealed that all but one model parameter were well-identified, and it is possible

to quantify the uncertainties of the model predictions of the response components.

10. Estimation of Henry- and mass transfer from ozone self-decomposition runs in water

10.1 Modified Beltrán method for estimation of Henry's coefficient and mass transfer

In this study, the ozone gas-liquid mass transfer into water in a bubble column was investigated for different pH values. The ozone volumetric mass transfer coefficient and the Henry's coefficient were determined simultaneously by parameter estimation using a nonlinear optimization method.
The bubble column was operated as a semi-batch reactor. The experimental set-up is presented in Fig. 10.1

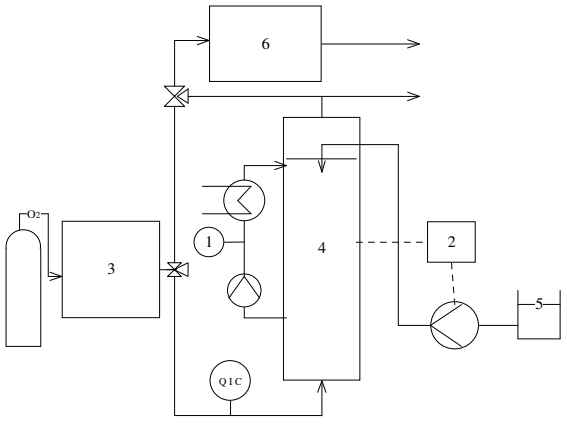

Figure 10.1 Experimental set-up: 1. Ozone sensor, 2. pH control, 3. Ozone generator, 4. Column, 5. Tank for pH adjustment liquid, 6. Spectrophotometer

10.1.1 Model equations

The algebraic model of the chemisorption process is presented in the form of the following equation (Beltrán et al., 1996):

$$P_{O_3 o} = \frac{P_{O_3 i}}{\exp\left[\frac{k_L a P_T h_T S}{H m_T}\right]} + \left[H - \frac{H}{\exp\left[\frac{k_L a P_T h_T S}{H m_T}\right]}\right] C_{O_3} \qquad (10.1)$$

In equation 10.1, C_{O_3} is the ozone concentration in the liquid phase and $P_{O_3 i}$ and $P_{O_3 o}$ are the ozone partial pressures in the gas phase in the inlet and outlet, respectively. P_T is the overall pressure, m_T total molar flow rate of the gas, h_T the height of the column and S the cross-sectional area of the column. The equation 10.1 presumes ideal plug flow of the gas phase and the perfect mixing of the water phase, which is a quite good approximation of the behavior of contactors similar to that used in this study (Towell et al., 1965). It also must be assumed that the reaction is slow. The Hatta number was < 0.02 for first order reaction, calculated from the equation presented by W. J. Masschelein(2000). Sometimes the ozone self-decomposition reaction is considered to be of the second reaction order. In that case Ha is < 0.3. When equation 10.1 was used for the estimation of $k_L a$ and H, the superficial velocity of the gas was 0.0164 m/s.

Instead of plotting C_{O_3} against $P_{O_3 o}$, $k_L a$ and H are estimated by comparing the measured and predicted $P_{O_3 o}$ calculated from the measured $C_{O_3 o}$ with changing input gas concentrations $P_{O_3 i}$ and gas flow rates. In Beltrán et al. method they both should be constant.

The volumetric mass transfer coefficient depends mainly on the gas superficial velocity, and a correlation of a general form can be written as

$$k_L a = B_1 \left(\frac{U}{U_{ref}} \right)^{B_2} \qquad (10.2)$$

The gas superficial velocity, U, was divided by U_{ref} to improve the identifiability of the parameters. U_{ref} can be chosen freely, but its magnitude is generally the same as that of U. In this study, an average gas velocity of 0.0160 m/s was used as the value of U_{ref}. When equation 10.1 was used with equation 10.3, the parameters B_1, B_2 and H were estimated.

The Henry's law coefficient can be written as a function of pH according to equation 10.3

$$H = B_3 \left(\frac{pH}{pH_{ref}} \right)^{B_4} \qquad (10.3)$$

where pH_{ref} is a reference pH value. In this study pH 7.0 was used as the reference value. Equation 10.3 was inserted into equation 10.1 along with equation 10.2 and the parameters B_1, B_2, B_3 and B_4 were estimated.

10.1.2 Results and discussion

The Henry's law constant and volumetric mass transfer coefficients were determined at pH levels of 4, 6, 7, 8, 9, 10 and 11 when the model of equation 10.1 was used and at pH levels of 4, 7 and 9 when the model of equations 10.1 and 10.2 was used. The Henry's coefficients obtained by using equation 10.1 are shown in Fig. 10.2 and in Table I in Appendix I. It can be seen that the apparent Henry's coefficient is increasing as function of the pH level from pH 7 to 11. The difference between the estimated Henry's coefficients and the value calculated using the equation of Roth and Sullivan (1981) varies between 7.4 and 28 %. The Henry's coefficients obtained by using the model of equations 10.1 and 10.2 are also shown in Fig. 10.2 and in Table in Appendix I. In this case, no significant correlation between the pH level and H can be found. The curve of correlation equation 10.3 (corr. of equations 10.1, 10.2 and 10.3) is also presented in Fig. 10.2.

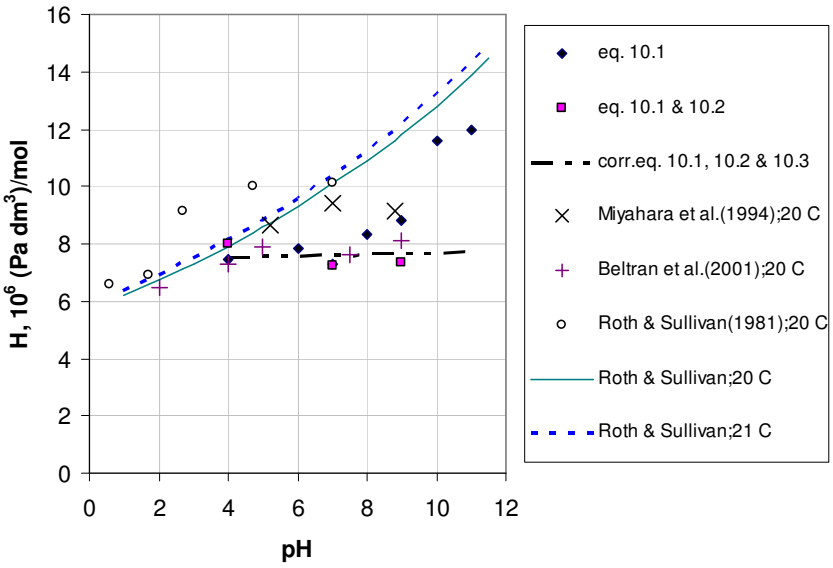

Figure 10.2. Henry's coefficient of ozone in 21 °C water.

The $k_L a$ computed with different data are compared to literature equations in figure 10.3.

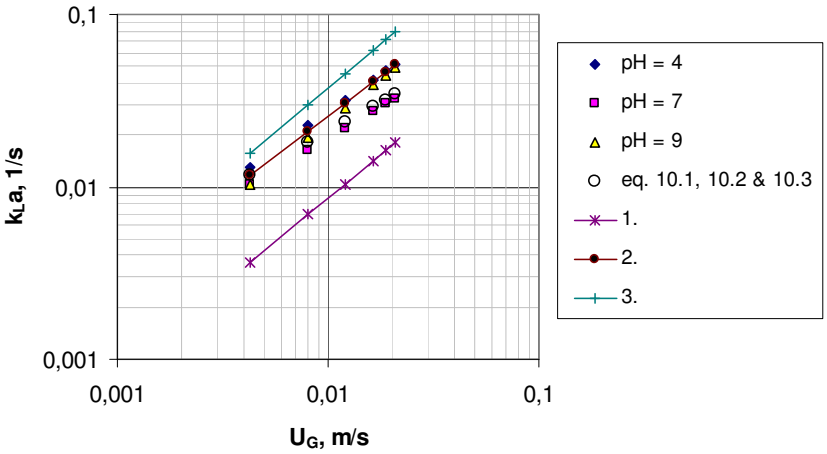

Figure 10.3. Volumetric mass transfer coefficients of ozone in 21 °C water solution predicted with the use of the model of equations 10.1 and 10.2. The k_La values of the model equation 10.2 with the parameters estimated from the model of equations 10.1, 10.2 and 10.3 are shown. The lines 1. $k_La=0.867U$, 2. $k_La=1.89U^{0.932}$ and 3. $k_La=4.12U^{1.02}$ of 25 °C come from the data of different authors presented by Bin and Roustan (2000).

The estimated parameters, the standard errors and correlation matrices of the models of equations 10.1 and 10.1 and 10.2 and the sensitivity contour plots for these models can be seen in Appendix I.

Two of the sensitivity contour plots of the objective function $l(B_1,B_2,B_3,B_4)$ are shown in figure 10.4.

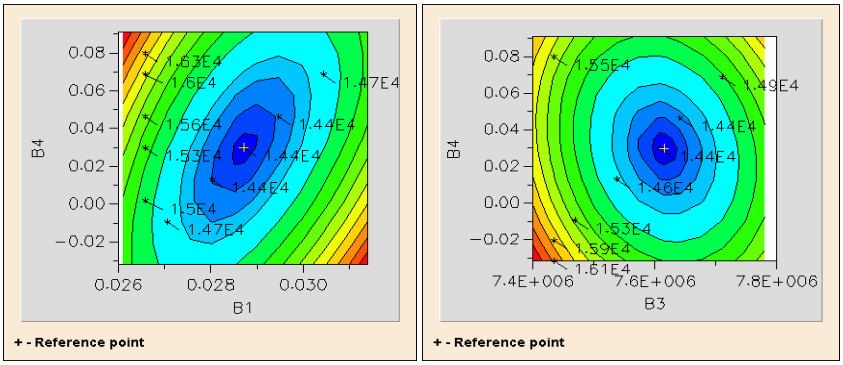

Figure 10.4 The sensitivity contour plots of function $l(B_1, B_2, B_3, B_4)$.

The coefficient of determination of the model of the equations 10.1, 10.2 and 10.3 was 98.37 %. In Table 10.1, the estimated parameters B_1, B_2, B_3, B_4, standard errors and relative standard errors of the parameters are shown. The off-diagonal elements of the correlation matrix obtained with the use of the model of equations 10.1, 10.2 and 10.3 are shown in table 10.2.

Table 10.1 **Estimated parameters B_1, B_2, B_3, B_4, standard errors and relative standard errors of the parameters obtained with the use of the model of equations 10.1, 10.2 and 10.3.**

Parameter	value	σ	σ, %
B_1	0.0287	0.00106	3.7
B_2	0.675	0.0360	5.3
B_3	$7.616\ 10^6$	$6.52\ 10^4$	0.9
B_4	0.0297	0.0245	82.8

Table 10.2 **Off-diagonal elements of the correlation matrix obtained with the use of the model of equations 10.1, 10.2 and 10.3.**

r_{ij}		
0.510		
0.613	0.141	
0.533	0.075	0.274

In figure 10.4 the sensitivity contour plots of the model of equations 10.1, 10.2 and 10.3 are well centered around the minimum point of the least squares function. The plots (B_1,B_2), (B_1,B_3), (B_2,B_3) and (B_2,B_4) which are not presented here are very similar to plots (B_1,B_4) and (B_3,B_4). From table 10.2 one can deduce that the values of the correlation matrix of the model of equations 10.1, 10.2 and 10.3 are the best ones in this study (Appendix I). Taking into consideration the standard error of the parameter B_4 presented in table 10.2, it seems that the Henry's law constant changes slightly as a function of pH.

10.2.3 Conclusion for chapter 10

The aim of this research was to determine the Henry's coefficient of ozone in water and the volumetric mass transfer coefficient at different levels of pH. The parameter estimation method developed in this study offers a different and practicable method to determine these constants. Furthermore, in contrast to the Beltrán method, the ozone concentration at the inlet of the reactor does not need to be constant. This method is also general, suitable for "pure" water and water solutions with organics or other with ozone reactive components. The Henry's coefficients and the volumetric mass transfer coefficients obtained during this research are of the same magnitude as the results in literature. It is important that the model parameters are dependent on each other as little as possible. The identifiability of the model was improved by conducting the experiments at different gas velocities. The most reliable result was obtained when the k_La values were presented as a function of superficial gas velocity and the Henry's coefficient as a function of pH. In this case, all the correlation parameters were well identified and did not correlate with each other. When

considering the estimated standard errors it seems that at the pH range 4–9 the Henry's coefficient is only marginally, if at all dependent on the pH value.

11. Axial dispersion model for estimation of ozone self-decomposition

A new method using the axial dispersion model for estimation of ozone self-decomposition kinetics in a semibatch bubble column reactor was developed. The reaction rate of ozone decomposition and the gas phase dispersion coefficient were estimated and compared with literature data. The experimental set-up was similar to that presented in Fig. 10.1.

11.1 Model equations

The axial dispersion model (ADM) was chosen to describe the gas dispersion and the hydrodynamics of the liquid and gas phases. The model consisted of a system of partial differential equations 11.1–11.3 including ozone mass transfer as well as the ozone self-decomposition.

$$\varepsilon_G \frac{\partial [O_3]_G}{\partial t} = -U_G \frac{\partial [O_3]_G}{\partial z} - k_L a\left([O_3]^* - [O_3]_L\right) + \varepsilon_G E_G \frac{\partial^2 [O_3]_G}{\partial z^2} \quad (11.1)$$

$$(1-\varepsilon_G)\frac{\partial [O_3]_L}{\partial t} = k_L a\left([O_3]^* - [O_3]_L\right) - r_{O_3} + (1-\varepsilon_G)E_L \frac{\partial^2 [O_3]_L}{\partial z^2} \quad (11.2)$$

$$\frac{\partial [O_3]_G}{\partial t} = -U_G \frac{\partial [O_3]_G}{\partial z} + E_{GT} \frac{\partial^2 [O_3]_G}{\partial z^2} \quad (11.3)$$

In the parameter estimation the partial differential equations 11.1-11.3 were solved numerically and integrated by the method of lines presented by Schiesser and Silebi (1997) with the following initial and boundary conditions.

$$t = 0, \quad 0 \le z \le L \qquad [O_3]_L = 0, \quad [O_3]_G = 0 \quad (11.4)$$

$$t > 0, \qquad \left.\frac{\partial [O_3]_G}{\partial z}\right|_{Z=0} = \left.\frac{\partial [O_3]_G}{\partial z}\right|_{Z=1.3m} = \left.\frac{\partial [O_3]_G}{\partial z}\right|_{Z=L} = 0, \qquad [O_3]_G|_{Z=0} = [O_3]_{Ginlet}(t) \quad (11.5)$$

$$t > 0, \qquad \left.\frac{\partial [O_3]_L}{\partial z}\right|_{Z=0} = \left.\frac{\partial [O_3]_L}{\partial z}\right|_{Z=1.3m} = 0 \quad (11.6)$$

Equation 11.3 applies to the gas phase of the column above the gas-liquid zone(head space).

The volumetric mass transfer coefficient depends mainly on the gas superficial velocity. A correlation of the general form can be written as

$$k_L a = B_1 \left(\frac{U_G}{U_{Gref}} \right)^{B_2} \qquad (11.7)$$

U_G, is divided by a reference velocity U_{Gref}. U_{Gref} can be chosen freely, but its magnitude is generally the same as that of U_G. In this study, an average gas velocity of 0.0160 m/s was used as the value of U_{Gref}. Using the equation including the reference value for the variable helps to make the estimated coefficients of the equation more independent. When equation 11.7 is used with equations 11.1 and 11.2, the parameters B_1 and B_2 are those estimated in an earlier work (Appendix I). In that work it was shown that the small amounts of NaOH used in the experiments have relatively small effect on $k_L a$. With a superficial gas velocity range 0.0042-0.021 m/s and a pH range of 7.0-11.0 estimated standard errors σ_{B1}=3.7 % and σ_{B2}=5.3 % were obtained.

The pseudo-Henry's law coefficient can be written as a function of pH according to the following equation

$$H = B_3 \left(\frac{pH}{pH_{ref}} \right)^{B_4} \qquad (11.8)$$

where pH_{ref} is a reference pH value. As well as B_1 and B_2, B_3=7.161 10^6 and B_4=0.0297 were estimated in an earlier work (Appendix I).

The goal of this part of the study was to compare, using an ADM model how well different kinetic models of ozone self-decomposition published in literature described the observed ozone concentrations in our experiments with very different hydrodynamics compared to the earlier self-decomposition studies. The observed values are the ozone concentration in the gas phase at the outlet of the column and the ozone concentration in the liquid phase.

Table 11.1 Kinetic models used for comparison. k_1 is specific to the chemical composition of the aqueous system.

Model eq.	Eq. number	Valid pH range	Author
$r_{O_3} = k_1[O_3]^2[OH^-]^{0.55}$	11.9	2-9.5	Gurol and Singer (1982)
$r_{O_3} = k_1[O_3][OH^-]^{0.75}$	11.10	7.6-10.4	Stumm (1954)
$r_{O_3} = k_A[O_3] + k_B[OH^-]^{1/2}[O_3]^{3/2}$	11.11	Acidic and basic	Sotelo et al. (1987)

The ozone self-decomposition reaction rate in this research was also described by the equation of the most common form in ozonation with reaction orders k_2, k_3 , with the exception that the concentrations of ozone $[O_3]$ and the hydroxyl ion $[OH^-]$ were divided by their reference values

$$r_{O_3} = k_1\left(\frac{[O_3]}{[O_3]_{ref}}\right)^{k_2}\left(\frac{[OH^-]}{[OH^-]_{ref}}\right)^{k_3} \qquad (11.12)$$

The reference values $[O_3]_{ref}$ = 1.126 10^{-6} mol/dm^3 and $[OH^-]_{ref}$ = 1.0 10^{-7} mol/dm^3 were used.

In equation (11.1) the gas dispersion coefficient is presented as a linear function of the gas superficial velocity.

$$E_G = B_5\left(\frac{U_G}{U_{Gref}}\right) \qquad (11.13)$$

The gas dispersion coefficient in equation 11.3 for the top of the column is written in a similar way

$$E_{GT} = B_{10}\left(\frac{U_G}{U_{Gref}}\right) \qquad (11.14)$$

The liquid phase dispersion coefficient was estimated by using the correlation equation by Baird and Rice (1975).

$$E_L = 0.35\, d_R^{4/3} (g\, U_G)^{1/3} \qquad (11.15)$$

Some more recent data on E_L have been given in the paper by Bińet al. (2001). Typical values (very scattered) are of the order of 10^{-2} m^2/s for U_G < 0.05 m/s.

Coefficients k_1, B_5 and B_{10} or k_A, k_B, B_5 and B_{10} or coefficients k_1, k_2, k_3, B_5 and B_{10} were determined simultaneously by nonlinear parameter estimation. A sensitivity analysis was conducted to obtain information on the reliability and identifiability of the estimated parameters.

11.2 Results and discussion

The values of the coefficients k_1 B_5 and B_{10}, were estimated by using kinetic equations 11.9 and 11.10 in the cases: E_L was calculated from equation 11.15, E_L = 0 which means no axial dispersion in the liquid side, and $E_L = 10^6(U_G/U_{Gref})$ which means very vigorous mixing in the liquid side. The values of the coefficients k_A, k_B, B_5 and B_{10} as well as the values of the coefficients k_1, k_2, k_3, B_5 and B_{10} were estimated in the case of $E_L = 10^6(U_G/U_{Gref})$.

The estimated values of the coefficients B_5, B_{10}, k_1, standard deviations, coefficient of determinations (the R^2 values) and the off-diagonal terms of approximate correlation matrices are presented and the estimated values of the coefficients k_A, k_B, B_5 and B_{10}, standard deviations, coefficient of determinations and the

off-diagonal terms of approximate correlation matrices are presented in Appendix II.

Table 11.2 lists the estimated values of the coefficients k_1, k_2, k_3, B_5 and B_{10}, standard deviations, coefficient of determinations and Table 11.3 gives the off-diagonal terms of the approximate correlation matrix of the case of equation 11.12.

Table 11.2 Estimated values of coefficients k_1, k_2, k_3, B_5 and B_{10}, standard deviations, coefficient of determinations in the case of equation 11.12.

Kinetic eq.	E_L $\frac{m^2}{s}$	k_1 10^{-8}	σ_{k1} %	k_2	σ_{k2} %	k_3	σ_{k3} %	B_5 $\frac{m^2}{s}$	σ_{B5} %	B_{10} $\frac{m^2}{s}$	σ_{B10} %	R^2 %
11.12	$10^6\left(\frac{U_G}{U_{G\,ref}}\right)$	1.09	2.4	1.123	2.2	0.508	1.3	0.0101	2.3	0.0035	1.1	97.20

Table 11.3 Off-diagonal terms of the approximate correlation matrix in the case of equation 11.12.

$r_{i\,j}$			
-0.013			
0.043	0.090		
0.534	-0.038	0.022	
0.140	0.144	-0.093	-0.448

In all cases the standard errors of the parameters are remarkably low (see Appendix II) and all off-diagonal terms of the correlation matrices are well below 0.9, which shows low interaction between the estimated parameters of the model. The coefficient of determination is improved when the liquid dispersion coefficient was set high. It can be also deduced (Appendix II) that the off-diagonal term r_{1N} of the correlation matrix is at its lowest value when the gas dispersion coefficient is high. The second best coefficient of determination 97.13 % is reached when the kinetic model equation 11.11 is used and the liquid dispersion coefficient has a value 10^6 (U_G/U_{Gref}). The best coefficient of determination 97.20 % is attained in the case of kinetic equation 11.12.

The reaction rates from literature and reaction rates obtained during this study are presented in figure 11.1.

It can be seen that, depending on pH, the reaction rates obtained by Sullivan and Roth (1980)(except at pH 7), Sotelo et al.(1987) and Hsu et al. (2002) are a little or remarkably lower than those of this study. The difference could come from the use of phosphate buffers in their experiments. Also the reaction rate at pH 7.0 of Gurol and Singer (1982) has been attained when using phosphate buffer. Gurol and Singer showed that phosphate has a significant retardation effect on the rate of ozone decomposition. Phosphate acts as a hydroxyl radical ($OH^{\bullet}$) scavenger (Gurol and Singer,

1982), which explains the icreasing difference between the results as function of pH. The reaction rate coefficient depends on the additives in the solution and also on the ionic strength. It must be noted that the ionic strength used in this study (Table III) was very low compared to most ozone self-decomposition research available in literature where it is typically in the range 0.01-0.15. In Fig. 11.1 the reaction rates of Gurol and Singer (1982) have been calculated by using their rate constants k_d obtained for the equation $r_{O_3} = k_d[O_3]^n$ with n = 2 at different pH values of water. However, equation 11.9 with the rate constant obtained in this study gives a considerably higher self-decomposition rate as a function of pH.

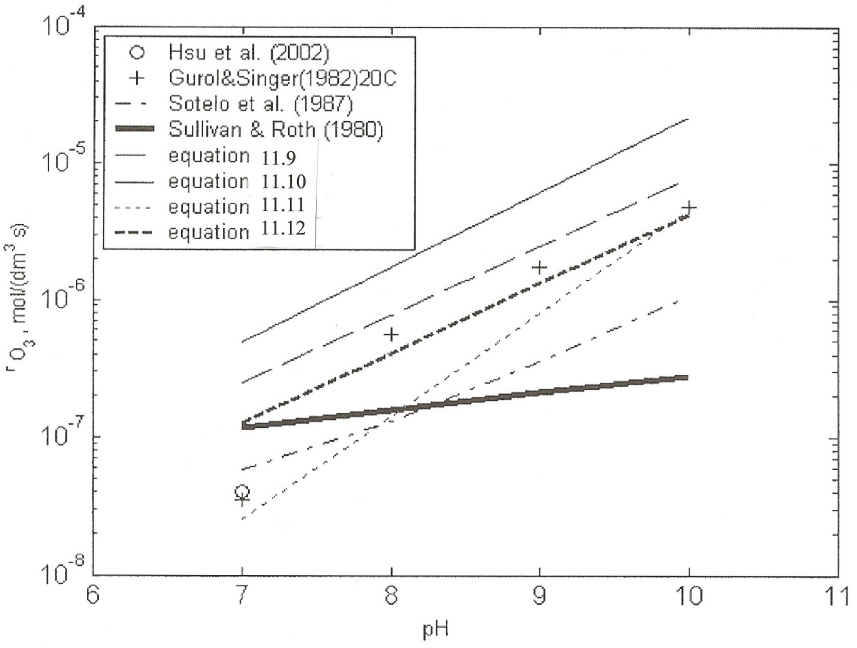

Figure 11.1 Reaction rate of ozone self-decomposition in 21 ºC water. Ozone concentration is 10^{-4} mol/dm^3. The reaction rate coefficients of equations 11.9 –11.12 are for the case $E_L=10^6$ (U_G/U_{Gref}).

The two-dimensional contours of the objective function $l(\beta)$ are given in Appendix II.

$$l(\beta) = \left\| y - y_p \right\|^2 = \sum_{i=1}^{n} (y_i - y_{ip})^2 = \sum_{i=1}^{n/2} \left(\left([O_3]_{GO} - [O_3]_{GOp} \right)^2 + \left([O_3]_L - [O_3]_{Lp} \right)^2 \right) \qquad (11.16)$$

The contours of the objective functions $l(B_5, k_A)$, $l(B_{10}, k_A)$ and $l(k_A, k_B)$, (see Fig. 11.2) revealed that a sufficiently small change in k_A does not affect the estimated value of k_B at a pH range above 7

as it was expected. The contours of the objective functions $l_{(k_2,k_3)}$, $l_{(k_3,B_5)}$ in the case of kinetic Equation 11.12 are presented in Fig. 11.13. The contours $l_{(k_2,B_5)}$, $l_{(k_3,B_{10})}$, $l_{(k_2,B_{10})}$, $l_{(k_1,B_{10})}$, $l_{(k_1,B_5)}$, $l_{(k_1,k_3)}$ and $l_{(k_1,k_2)}$, which are not shown here, are very similar to $l_{(k_2,k_3)}$ or $l_{(k_3,B_5)}$.

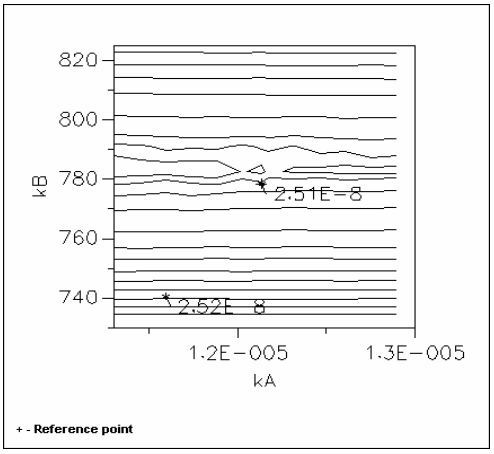

Figure 11.2 Contour of the objective function $l_{(k_A,\ k_B)}$. Kinetic model equation 11.11 is used and the liquid dispersion coefficient is 10^6 (U_G/U_{Gref}).

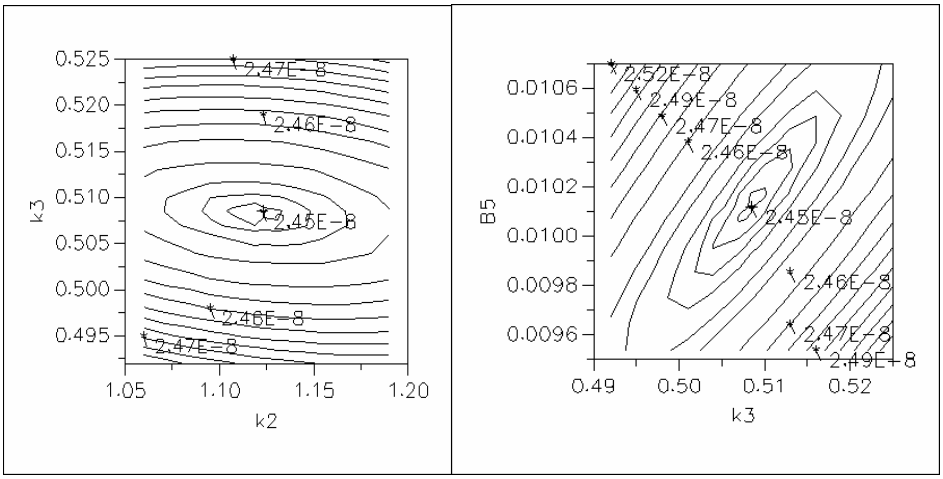

Figure 11.3 Contours of the objective function l (k_2, k_3) and l (k_3, B_5). Kinetic model equation 11.12 is used and the liquid dispersion coefficient is 10^6 (U_G/U_{Gref}).

11.3 Conclusion for chapter 11

In this study, a new method was developed to estimate ozone self-decomposition kinetics from a semi-batch bubble column. Plug flow, perfectly mixed models and axial dispersion models were used in the liquid phase and an axial dispersion model was used in the gas phase. The position of the dissolved ozone sensor was taken into account.

Four reaction rate equations were used for estimation of the reaction rate constants of ozone self-decomposition and gas phase dispersion coefficients. The coefficient of determination always tended to improve when the liquid dispersion coefficient was set high, which means vigorous mixing in the liquid phase was assumed. The second best fit was attained when the kinetic equation of Sotelo et al.(1987) was applied. The best fit was attained when the kinetic equation with the reaction orders of ozone and hydroxyl ion were applied as estimated parameters, resulting in a

reaction order 1.12 for ozone and 0.51 for the hydroxyl ion in the pH range 7–10. In this case as well as with the kinetic models of Gurol and Singer (1987) and Stumm (1954) the parameters were well identified and did not correlate with each other.

12. Estimation of mass transfer and multi component reaction kinetics of p-nitrophenol ozonation in a bubble column

The reaction rate coefficients and the stoichiometric coefficients in the reaction of ozone with the model component p-nitrophenol at a low pH of aqueous solution were estimated by using nonlinear optimization. Two kinds of experimental runs were performed: runs with pH 2.0 and runs without pH adjustment. The reaction rate equations were written by applying a modified reaction scheme of Yu and Yu (2001) (Fig. 12.1). The concentration of the unknown intermediate compounds is given as residual COD calculated from the measured COD and theoretical COD for the known species as shown in chapters 8.2.3 and 8.2.4.

In the reaction scheme of p-nitrophenol ozonation there are two main reaction pathways from p-nitrophenol. One pathway is via the intermediates 4-nitrocathecol and catechol to volatile acids and the other pathway is via hydroquinone and p-quinone. In Figure 12.1 COD_{res} represents the residual COD of the intermediate species, that is the measured total COD from which the theoretical COD of p-nitrophenol and hydroquinone have been subtracted.

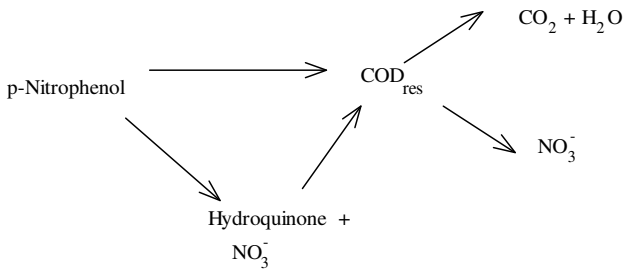

Figure 12.1 Reaction scheme of p-nitrophenol ozonation.

12.1 Experimental set-up

The bubble column was operated as a semi-batch reactor. The data from experimental runs without pH adjustment were collected using a spherical column and a rectangular column was used for the constant pH 2 runs. The gas was fed into the column from the bottom through a porous plate. The gas phase ozone concentration is measured at the inlet and the outlet of the column, but the ozone or the intermediate concentration in the liquid phase is measured only at one point in the domain and perfect mixing is assumed. The ozone and intermediate concentrations of the liquid phase were analyzed. More detailed information about the experimental conditions and the analysis of the samples can be found in Appendixes III and IV.

12.2 Model equations for mass transfer and hydrodynamics

The axial dispersion model (ADM) was chosen to describe the gas dispersion and the hydrodynamics in the gas phase, and the CSTR model was used for the liquid phase. According to an earlier study (Appendix II), complete mixing on the liquid side could be assumed at the used gas superficial velocity of 0.0160 m/s. As the gas flow was relatively small, effectively plug flow of the gas phase can be assumed. The model consisted of a system of partial differential equations 12.1–12.3 including mass transfer and reaction.

For ozone in the gas phase,

$$\varepsilon_G \frac{\partial [O_3]_G}{\partial t} = -U_G \frac{\partial [O_3]_G}{\partial z} - N_{O_3} + \varepsilon_G E_G \frac{\partial^2 [O_3]_G}{\partial z^2} \qquad z < 1.3\,m \qquad (12.1)$$

For all components in the liquid phase, N_i = 0 for organics, or for NO_3^- .

$$(1-\varepsilon_G)\frac{\partial [i]_L}{\partial t} = N_i - (1-\varepsilon_G) r_i \qquad z < 1.3\,m \qquad (12.2)$$

For ozone in the gas phase in the head space,

$$\frac{\partial [O_3]_G}{\partial t} = -U_G \frac{\partial [O_3]_G}{\partial z} + E_{GT} \frac{\partial^2 [O_3]_G}{\partial z^2} \qquad 1.3 < z < 2.05\,m \qquad (12.3)$$

[i] represents the concentration of each component i. The gas above the liquid surface was estimated to have mixed tank conditions. The partial differential equations 12.1–12.3 were solved numerically in the parameter estimation and integrated by

the method of lines presented by Schiesser and Silebi (1997) with the following initial and boundary conditions;

$$t = 0, \quad 0 \le z \le L \qquad [O_3]_L = 0, \quad [O_3]_G = 0 \tag{12.4}$$

$$t > 0, \qquad \left.\frac{\partial [O_3]_G}{\partial z}\right|_{Z=0} = -U\,\frac{([O_3]_{Ginlet} - [O_3]_{calc})}{E_G}, \qquad [O_3]_G\big|_{Z=0} = [O_3]_{Ginlet}(t) \tag{12.5}$$

$$t > 0, \qquad \left.\frac{\partial [O_3]_G}{\partial z}\right|_{Z=L} = 0$$

$$t > 0, \qquad \left.\frac{\partial [i]_L}{\partial z}\right|_{Z=0} = \left.\frac{\partial [i]_L}{\partial z}\right|_{Z=1.3m} = 0 \tag{12.6}$$

Equation 12.3 applies to the gas head space on the top of the column. In equation 12.5 $[O_3]_{calc}$ is the computed concentration in the first cell on the gas side using the method of lines.

The reaction is assumed to take place dominantly in liquid bulk. N_{O_3} is obtained from the equation

$$N_{O_3} = k_L a \sum_{1}^{n} \left([O_3]_i^* - [O_3]\right) \tag{12.7}$$

where n=10 is the number of units on the gas side. The volumetric mass transfer coefficient k_La =0.042 m/s was obtained by the Beltran method (Beltrán et al., 1997).

13.3 The p-nitrophenol reaction model

The reactions 8.76 and 8.77 can be expressed as COD using the theoretical oxygen consumptions for NP and HQ calculated from their molecular structure and the residual COD calculated on the principle explained earlier in chapter 8.2.4

$$NP + \frac{2}{3} O_3 \xrightarrow{k_1} HQ + NO_3^- \quad (12.8)$$

$$\gamma_{NP} NP + \gamma_1 O_3 \xrightarrow{k_2} COD_{res} \quad (12.9)$$

$$\gamma_{HQ} HQ + \gamma_2 O_3 \xrightarrow{k_3} COD_{res} \quad (12.10)$$

$$\frac{3}{2} COD_{res} + O_3 \xrightarrow{k_5} CO_2 + H_2O \quad (12.11)$$

$$COD_{res} + \frac{2}{3} O_3 \xrightarrow{k_6} 2NO_3^- \quad (12.12)$$

$$O_3 \xrightarrow{k_4, k_7} \frac{3}{2} O_2 \quad (12.13)$$

The reaction rate equations 12.15-12.19 were written in the following mode presented in chapter 8.2.4

$$r_i = -\frac{d[i]}{dt} = \sum_{i \neq O_3} k_i \gamma_i [O_3][i] \quad (12.14)$$

γ_i represents the stoichiometric or theoretical coefficient.

$$r_{NP} = -\frac{d[NP]}{dt} = k_1[O_3][NP] + k_2[O_3][NP] \quad (12.15)$$

$$r_{HQ} = -\frac{d[HQ]}{dt} = -k_1[O_3][NP] + k_3[O_3][HQ] \quad (12.16)$$

$$r_{COD_{res}} = -\frac{d[COD_{RES}]}{dt} = -k_2(\gamma_{NP} - \gamma_1 \frac{3}{2})[O_3][NP] - k_3(\gamma_{HQ} - \gamma_2 \frac{3}{2})[O_3][HQ] +$$

$$k_5 \frac{3}{2}[O_3][COD_{res}] + k_6[O_3][COD_{res}] \quad (12.17)$$

$$r_{NO_3} = -\frac{d[NO_3]}{dt} = -k_1[O_3][NP] - k_5 2[O_3][COD_{res}] \quad (12.18)$$

$$r_{O_3} = -\frac{d[O_3]}{dt} = k_1 \frac{2}{3}[O_3][NP] + k_2\gamma_1[O_3][NP] +$$

$$k_3\gamma_2[O_3][HQ] + k_4[O_3][NP] + k_5[O_3][COD_{res}] + k_6\frac{2}{3}[O_3][COD_{res}] + k_7[O_3][HQ] \quad (12.19)$$

The parameters γ_{NP} = 7.25 mol O_2/mol NP and γ_{HQ} = 6.5 mol O_2/mol HQ represent the theoretical COD of p-nitrophenol and hydroquinone, respectively.

12.4 Parameter Estimation

The reaction rate coefficients k_i and the stoichiometric coefficients γ_i and the mass transfer coefficient were obtained by parameter estimation using Modest 6.0 parameter estimation software (Haario 1994). In parameter estimation, the objective function was the weighted sum of the squares of the residuals between the model and the data

$$l(\beta) = \left\| y - y_p \right\|^2 = \sum_{i=1}^{n} (y_i - y_{ip})^2 w_i \quad (12.20)$$

where y_i represents the measured concentration of component i. The y_{ip} for the total COD was computed according to the following equation

$$y_{CODp} = [COD_{res}] + \gamma_{NP}[NP] + \gamma_{HQ}[HQ] \quad (12.21)$$

The other concentrations y_i were ozone concentration in the gas phase at the outlet of the column, dissolved ozone, p-nitrophenol, hydroquinone and NO_3^- concentrations.

12.4 Results and discussion

The rate coefficients obtained by nonlinear parameter estimation, stoichiometric coefficients and mass transfer coefficients are presented in table 12.1.

Table 12.1 Estimated values for the experimental parameters

Parameter, dimension	Estimated value pH 2	Estimated STD *(relative)*	Estimated value, initial pH 5	Estimated STD *(relative)*
k_1, $\frac{dm^3}{mol\ s}$	97.2	23.7 *(24.3 %)*	71.5	8.81 *(12.3%)*
k_2, $\frac{dm^3}{mol\ s}$	104	21.4 *(23.9 %)*	31.6	4.18 *(9.0 %)*
k_3, $\frac{dm^3}{mol\ s}$	286	74.4 *(26.0 %)*	203	25.4 *(12.5 %)*
k_4, $\frac{dm^3}{mol\ s}$	9.17×10^{-3}	63.3 *(875×10^3 %)*	195	19.1 *(9.8 %)*
k_5, $\frac{dm^3}{mol\ s}$	8.32	0.44 *(5.4 %)*	10.1	1.28 *(12.6 %)*
k_6, $\frac{dm^3}{mol\ s}$	0.76×10^{-7}	6.35×10^{-3} *(83.1×10^4 %)*	1.60	0.34 *(21.0 %)*
γ_1	3.39	0.27 *(8.1 %)*	3.02	0.30 *(10.0 %)*
γ_2	1.26×10^{-3}	0.33 *(261×10^3 %)*	0.88×10^{-2}	1.6×10^{-5} *(2154 %)*
k_La, $\frac{1}{s}$	0.027	0.11×10^{-2} (4.0 %)	0.044	0.49×10^{-2} (11.1 %)

The correlation matrices calculated using the clasasical analysis and MCMC theory are presented in Tables 12.2 and 12.3. Only one or two of the matrices terms are higher than 0.9. On this basis it can bee deduced that the parameter values are reliable. It can be seen that the MCMC gives correlation matrix values that are slightly better (for example, for rate coefficients) or remarkably better (see those for $k_L a$) than classical analysis.

Table 12.2. Correlation matrices of the estimated parameters from classical statistical analysis (left) and from MCMC (right) using data obtained at pH 2

k_1	1.00								
k_2	0.86	1.00							
k_3	0.92	0.71	1.00						
k_4	-0.33	-0.22	-0.27	1.00					
k_5	-0.04	-0.05	-0.09	-0.19	1.00				
k_6	-0.17	-0.14	-0.15	0.05	-0.22	1.00			
k_La	-0.83	-0.81	-0.71	0.70	-0.07	0.09	1.00		
γ_2	0.25	-0.30	0.23	-0.15	-0.57	-0.003	-0.36	1.00	
γ_1	0.06	-0.34	0.15	0.06	0.18	0.164	0.22	-0.65	1.00
	k_1	k_2	k_3	k_4	k_5	k_6	k_La	γ_2	γ_1

k_1	1.00								
k_2	0.76	1.00							
k_3	0.88	0.58	1.00						
k_4	0.19	0.27	0.14	1.00					
k_5	0.23	0.29	0.15	-0.07	1.00				
k_6	-0.04	0.03	-0.04	0.05	-0.09	1.00			
k_La	-0.72	-0.76	-0.62	0.21	-0.46	-0.02	1.00		
γ_2	0.04	0.08	-0.03	-0.0004	0.01	0.04	-0.13	1.00	
γ_1	0.26	-0.38	0.34	-0.07	-0.22	-0.07	0.11	-0.17	1.00
	k_1	k_2	k_3	k_4	k_5	k_6	k_La	γ_2	γ_1

Table 12.3 Correlation matrices of the estimated parameters from classical statistical analysis (left) and from MCMC (right) using data at initial pH 5

k_1	1.00								
k_2	0.72	1.00							
k_3	0.97	0.68	1.00						
k_4	0.66	0.55	0.62	1.00					
k_5	0.59	0.44	0.58	0.16	1.00				
k_6	0.27	0.74	0.24	0.24	0.14	1.00			
k_La	-0.75	-0.70	-0.74	-0.07	-0.66	-0.42	1.00		
γ_2	0.24	0.27	0.24	0.32	-0.47	0.22	-0.09	1.00	
γ_1	0.07	-0.42	0.09	-0.10	0.37	-0.54	0.041	-0.73	1.00
	k_1	k_2	k_3	k_4	k_5	k_6	k_La	γ_2	γ_1

k_1	1.00								
k_2	0.46	1.00							
k_3	0.94	0.36	1.00						
k_4	0.92	0.74	0.84	1.00					
k_5	0.63	0.31	0.60	0.61	1.00				
k_6	-0.06	0.69	-0.10	0.25	-0.02	1.00			
k_La	0.24	0.25	0.27	0.20	0.22	0.15	1.00		
γ_2	0.03	0.06	-0.05	0.05	-0.24	0.03	-0.0008	1.00	
γ_1	0.40	-0.52	0.41	0.07	0.11	-0.67	-0.02	-0.29	1.00
	k_1	k_2	k_3	k_4	k_5	k_6	k_La	γ_2	γ_1

12.5 MCMC analysis in practice

The theory and the full MCMC analysis can be found in appendix IV. From the practical point of view, and on the basis of experience obtained during this research, it can be concluded that the MCMC analysis was very helpful in finding “true” parameter values. In parameter estimation for complex models which include a large amount of estimable parameters, it is difficult to find parameters that can be relied on. The classical statistical analysis may give good correlation matrices suggesting low interdependence between the estimated parameters and acceptable standard errors for all the parameters and those parameters may give very good fits for the data. However, MCMC analysis may reveal that only some of the

parameters are close enough to the optimum. In this research, typically, the parameter values suggested by MCMC analysis after the first nonlinear optimization were used as new initial guesses and a new optimization was performed. After this procedure, the newly found parameters suggested by nonlinear estimation were the same as that from the MCMC analysis.

12.6 Conclusion for chapter 12

Experimental data from p-nitrophenol ozonation at pH 2 was used to develop a novel kinetic model and to estimate the reaction kinetic parameters, taking into consideration gas-liquid mass transfer and the reactions between ozone, p-nitrophenol and intermediates. The decomposition rate of p-nitrophenol on the pathway producing hydroquinone was found to be almost equal to the decomposition rate on the pathway producing 4-nitrocatechol. Comparison of the rate coefficients for the case with initial pH 5 indicated that the p-nitrophenol degradation producing 4-nitrocathecol was more selective towards molecular ozone than the reaction producing hydroquinone. The model introduced for ozone consumption was solved numerically using the stoichiometric ozone demand and an additional term of ozone decomposition. On the basis of data obtained from the experimental runs and the sensitivity analysis it can be deduced that the developed model works properly and can be used to obtain reliable reaction kinetic parameters. The consumption of ozone was found to be about 5 mol of O_3 per mol of

p-nitrophenol degraded. In the parameter estimation, the model provided parameters that simulated the process well and supported the results found in the literature as regards the reaction rate and reaction scheme of p-nitrophenol ozonation. The ozone reaction decomposing the residual COD to CO_2, representing reactions with several different intermediates, both with species reacting with ozone relatively fast and those reacting slowly (volatile acids), was identified well on the basis of the statistics.

MCMC analysis was carried out to study the reliability of the estimated parameters and the model predictions. The MCMC analysis was found to be useful in getting qualitative and quantitative information about the accuracy and reliability of the parameter estimation. In the cases studied, the MCMC analysis revealed that all except two of the model parameters were well-identified. MCMC analysis was able to quantify the uncertainties of the model predictions of the response components.

14. Conclusions

This thesis considers modeling of ozonation. In the literature part, estimation of mass transfer and reaction kinetics and reactions of ozone were discussed. As a result of this work a new and more general method based on Beltrán method was developed for estimation of the Henry's coefficient and mass transfer. In addition a method was developed for estimation of reaction

kinetics and the mass transfer coefficient based on the axial dispersion model. This method was also found useful in estimation of the dispersion of phases in a bubble column. Finally, a novel method based on residual COD was developed for estimation of reaction rate coefficients and stoichiometric coefficients in a multicomponent reaction system.

From the survey of ozonation literature it can be concluded that dealing with multicomponent ozonation reactions is not fully developed in everyday practice, especially, if organic species are involved. Much further research is needed to establish the usability of the radical chain method. The problem is the reliability of the numerous reaction kinetic parameters obtained from literature for a certain water solution. One solution could be the addition of sum parameters like COD, TOC and/or TIC to the radical chain reaction model. During this research a residual COD method was developed for estimation of reaction kinetics in multi component systems. In this novel method the number of parameters is relatively small, which helps to find reliable model parameter values. However, interpretation of the estimated stoichiometric coefficient for COD_{res} is not unambiguous resulting from the effect of polymerization and the effect of components that cannot be presented as COD for example, and therefore further experimental research and study of the applications of the method are desirable.

14. References

Akita, K., Yoshida, F., Gas holdup and volumetric mass transfer coefficient in bubble columns. Effects of liquid properties, Ind. Eng. Chem. Process. Des. Develop., 12(1),pp. 76-80 (1973)

Beck, J.V., Arnold, K.J., Parameter estimation in engineering and science, John Wiley and Sons: New York, (1977), p. 379

Beltrán, F.J., García-Araya J.F., Encinar,J. M., Henry and mass transfer coefficients in the ozonation of waste waters, Ozone Sci. Eng., 19 pp. 219-228 (1997)

Beltran, F.J, García-Araya, J.F., Álvarez, Domestic Waste Water Ozonation: A Kinetic Model Approach, Ozone Sci. Eng. 32,3, 219-228 (2000)

Beltrán, F.J, Gómez-Serrano, V., Durán, A., Degradation kinetics of p-Nitropehol ozonation in water, Wat. Res. Degradation kinetics of p-nitrophenol ozonation, 26(1) pp.9-17 (1992)

Benitez, J.F., Beltrán-Heredia, J., Acero, J.L., Rubio, J.F., Rate constants for the reactions of ozone with chlorophenols in aqueous solutions, Journal of Hazardous Materials, B79, pp. 271-285 (2000)

Bin, A., K., , Roustan, M., Mass transfer in ozone reactors, International specialized symposium, IOA 2000, Toulouse, France, 1-3 March (2000)

Charpentier, J.C.,Mass transfer rates in gas liquid absorbers and reactors, In: Advances in chemical engineering, Vol. 11, Drew, T.B., Hoopes, J.W., Vermeulen (ed.) Academic Press, New York, (1981), pp. 1-133

Chelkowska, K., Grasso, D., Fabian, I., Gordon, G., Numerical simulations of agueus ozone decomposition, Ozone Sci. Eng., 14(1), pp. 33-49 (1992)

Danckwerts, P.V., Gas liquid reactors, McGraw-Hill, New York, (1970)

García-Araya, J.,F. , Caracterizatión y tratamiento con ozono de aquas residuales de industrias alcoholeras y conserceras de tomate, Doctoral Thesis, University of Extremadura, Badajoz, (1993)

Gordon, G., The very slow decomposition of aquaeous ozone in highly basic solutions. Proc. 8th Ozone World Congress, IOA, Zürich, Switzerland (1987)

Gelman, A., Carlin, J., Stern, H., Rubin, D., Bayesian data analysis, second ed., Chapman Hall, London pp. 50-51 (1996)

Grasso, D., Ozonation dynamics in water treatment: Autocatalytic decomposition, Mass transfer and impact of particle stability. PhD dissertation, The University of Michigan, Ann Abor, Mich.(1987 a)

Von Gunten, Urs, Ozonation of drinking water: Part I. Oxidation kinetics and product formation, Water Research 37 pp. 1443-1467 (2003)

Gurol, M. D., Nekouinaini, S. Kinetic Behavior of Ozone in Aquaeous Solutions of Substituted Phenols, Ind. Eng. Chem. Fundam. 23, 54-60 (1984)

Gurol, M.D., Singer, P.C., Kinetics of ozone decomposition: A dynamic approach, Environ. Sci. Technol., 16 pp. 377-383(1982)

Haario, Modest users guide (1994)

Haario, H., Saksman, E., Tamminen, J., An adaptive Metropolis algorithm, Bernoulli, 7(2) pp. 223-242 (2001)

Hoigné, J., Bader, H., Ozonation of water: Selectivity and rate of oxidation of solutes. Proc. 3rd World Congress, Paris, France (1977 a)

Hoigné, J., Bader, H., Rate constants for reactions of ozone with organic pollutants and ammonia in water. IOA Symp., Toronto, Canada (1977 b)

Hoigné, J., Bader, H., Rate constants of reactions of ozone with organic and inorganic compounds in water-I. Non dissociating organic compounds, Water Res. 17, pp. 173-183 (1983 a)

Hoigné, J., Bader, H., Rate constants of reactions of ozone with organic and inorganic compounds in water-II. Dissociating organic compounds, Water Res. 17, pp. 185-194 (1983 b)

van Krevelen, D.W., Hoftijzer, P.J., Kinetics of gas liquid reactions. Part I. General theory, Recl. Trav. Chim. Pays-Bas, 67, pp.563-586(1948)

Kumar, R., Bose, P., Development and experimental validation of the model of a continuous-flow countercurrent ozone contactor, Ind. Eng., Chem. Res., 43, pp. 1418-1429 (2004)

Laplanche, A., Le Sauze, N., Martin, G., Langlais, B., Simulation of ozone transfer in water: Comparison with pilot unit, Ozone Sci. Eng., 13(5) (1991)

Lewis, W.K., Whitman, W.G, Principles of gas absorption Journal of Industrial and Engineering Chemistry (Wsashington D.C.) 16 pp.1215–1220 (1924)

Machelein, W.j:, Fundamental properties of ozone of ozone in relation in water sanitation and environmental applications, International Specialized Symposium, IOA 2000, Toulouse, France, 1–3 March, pp. 1–22 (2000)

Pedit, A.J., Iwamasa, K.J., Miller, C.T., Glaze, W.H., Development and application of a gas–liquid contactor model for simulating advanced oxidation processes, Environ. Sci. Technol. 31 pp. 2791–2796 (1997)

Pi, Y., Schumacher, J., Jekel, M., Decomposition of aquaeous ozone in the presence of aromatic organic solutes, Water Research 39, pp. 83–88 (2005)

Rao, 1978 Rao, S.S., Optimization theory and applications, Wiley Eastern Limited, New Delhi, India, p. 278 (1978)

Roth, J.A., Sullivan, D.E., Solubility of ozone in water, Ind. Eng. Fundam. 20 pp.337–344 (1981)

Roustan, M, Wang, R.Y., Wolbert, D., Modeling hydrodynamics and mass transfer parameters in a continuous ozone bubble column, Ozone. Sci. Eng., 18, pp. 99–115, (1996)

Schlüter, S., Steiff, A., Weinspach, P.,M., Heat transfer in two- and three–phase bubble column rectors with internals, Chemical Engineering and Processing, 33, 157–172 (1995)

Shiesser, W.E., Silebi, C.A., Computational transport phenomena, Cambridge University Press, Cambridge, U.K.,(1977)

Solonen, A., Montecarlo methods in parameter estimation of nonlinear models. Masters thesis, Lappeenranta University of Technology, Lappeenranta, Finland, (2006) (available online at http:/www.doria.fi/(collection LutPub))

Sotelo, J.L., Beltrán, F.J., Benitez, F.J., Beltrán–Heredia, Ozone decomposition in water: Kinetic study, Ind. Eng. Chem. Res. 26 pp. 34–43 (1987)

Staehelin, J., Hoigné, J., Decomposition of ozone in water: Rate of initiation by hydroxide ions and hydrogen peroxide, Environ Sci. & Technol., 16(10), pp. 676–681, (1982)

Staehelin, J., and Hoigné, J., Decomposition of ozone in water in the presence of organic solutes acting as promoters and inhibitors

of radical chain reactions, Environ. Sci. Technol., 19, pp. 1206-1213 (1985)

Stumm, W., The decomposition of ozone in drinking water, Helv. Chim. Acta, 37 pp. 773-778 (1954)

Tomiasu, H., Fukutomi, H., Gordon, G., , Kinetics and mechanism of ozone decomposition in Basic Aquaeous solution, Inorg. Chem., 24, pp. 2962-2966 (1985)

Towell, G.D., Strand, C.P., Ackerman, G.H., Mixing and mass transfer in large diameter bubble columns, Proc. AIChE-I. Chem. E., 10 pp. 97-105 (1965)

Weiss, J., Investigation on the radical HO_2 in solution, Trans . Faraday Soc., 31, 668-681 (1935)

Öztürk, S. S., Schumpe, A., Deckwer, W.-D., Organic Liquids in a Bubble Column: Holdups and Mass Transfer Coefficients, AIChE Journal, (33) 9, 1473-1480 (1987)

Yao, C.C.D., Haag, W.R., Mill, T., Kinetic features of advanced oxidation processes for treating aqueous chemical mixtures, in Proc. Of the 2nd Int. Symp. On Chemical Oxidation: Technologies for the nineties, Nashville, Tennesee, USA , 2, pp. 112-139 (1991)

Yurteri, C., Gurol, M.D., Ozone consumption in natural waters: Effects of background organic matter, pH and carbonate species, Ozone Sci. Eng., 10(3), 277-290 (1988)

Zou, H., Smith, D.W.,Stanley, S.W., Modeling dissolved ozone concentration profiles in Bubble columns, J. Environ. Eng. 120(4), pp. 821-840 (1994)

15. List of symbols

a	specific interfacial area in the unit volume of phase mixture, m^2/m^3
B_1, $B_{2,3,4,10}$	model parameters
b	parameter vektor
c	model constant
D, D_{O_3}	diffusion constant of ozone in the liquid, m^2/s
D_M	diffusion coefficient of solvent M, m^2/s
d_B	bubble diameter, m
d_R	column diameter, m
E_G	coefficient of axial dispersion in the gas phase, m^2/s
E_{GT}	coefficient of axial dispersion in the single phase flow, m^2/s
E_i	is the instantaneous reaction factor defined in the film theory
E_L	coefficient of axial dispersion in the liquid phase, m^2/s
g	function of s, gravitational constant, m/s^2
H	Henry law constant, $(Pa\ dm^3)/mol$
h_0	total height of the liquid surface without the passing gas, m
h_T	total height of the liquid surface with the passing gas, m
Ha	Hatta number
h_T	total height of the column with the passing gas, m
$J_{j,p}$	sensitivity coefficient
K_a	dissociation constant
k_A	reaction rate coefficient, 1/s
k_B	reaction rate coefficient, $dm^3/(mol\ s)$

k_d	reaction rate coefficient, $(dm^3/mol)^{n-1}/s$
k_L	individual liquid side mass transfer coefficient, m/s
k_La	volumetric mass transfer coefficient, 1/s
k_{m+n}	reaction rate constant of m+n th order
k_1	first order reaction rate coefficient, 1/s, reaction rate coefficient, $dm^3/(mol\ s)$
	reaction rate coefficient, $(dm^3/mol)^{n-1}/s$
k_2	reaction order of ozone, reaction rate coefficient, $dm^3/(mol\ s)$
k_3	reaction order of hydroxyl ion
l	objective function
$[M]_0$	initial concentration of M, mol/dm^3
m	reaction order for species M
n	reaction order of ozone
m_T	total molar flow rate, mol/s
N	number of estimable parameters
N_{O_3}	ozone mass flux, $mol/(m^3\ s)$
$[OH^-]$	hydroxide ion concentration, mol/dm^3
$[O_3]$	ozone concentration in the liquid phase, mol/dm^3
$[O_3]_G$	ozone concentration in the gas phase, mol/dm^3
$[O_3]_L$	ozone concentration in the liquid phase, mol/dm^3
$[O_3]^*$	saturation concentration of ozone in the liquid phase, mol/dm^3
pH_{ref}	reference value for the pH
pK	equilibrium constant
P_{O_3}	ozone partial pressure, Pa
$P_{O_3 i}$	ozone partial pressure at the column inlet, Pa

$P_{O_3 o}$	ozone partial pressure at the column outlet, Pa
P_T	total pressure, Pa
R	universal gas constant, 8,31441 J/(K mol)
R_{O_3}	is rate of of ozone mass transfer, g/(dm^3 s)
R^2	coefficient of determination
r_{O_3}	decomposition rate of ozone, mol/(m^3 s)
S	cross-sectional area of the column, m^2, solubility ratio
T	temperature, K
t	time, s
U_G	superficial velocity of the gas, m/s
$U_{G\,ref}$	reference value of the superficial velocity of the gas, m/s
V_R	reactor volume, m^3
V_G	volumetric flow of gas, m^3/s
V_L	volumetric flow of liquid, m^3/s
V_R	reactor volume, m^3
X	sensitivity matrix
x,x_j	experimental variable
Y	observation vector
y_i	observation
y_p	observed variable predicted by the model
$\bar{y}$	average value of all y_i
z	coordinate in direction of column height, m stoichiometrich coefficient

creek letters

α	degree of dissociation
β	estimated parameter, liquid hold-up
ε, ε_G	volumetric gas hold-up
ε_L	volumetric liquid hold-up
σ	standard deviation of the pure experimental error
γ	stoichiometric factor
ρ	density, kg/dm^3
μ	dynamic viscosity, Pa s

Subscripts

G	gas phase
i	inlet
o	outlet
ox	oxidated
L	liquid